# Effect of Processing, Dopant and Microwave Sintering on the Dielectric Properties of $BiFeO_3$ Ceramic

A Thesis Submitted in Partial Fulfilment of the
Requirements for the degree of

**Master of Technology**

in

**Ceramic Engineering**

by

**Uttam Kumar Chanda**

Under the Guidance of

**Dr. Ranabrata Mazumder**


**Department of Ceramic Engineering**
**National Institute of Technology**
**Rourkela**
**2013**

**Department of Ceramic Engineering**
**National Institute of Technology**
**Rourkela – 769008**
**Odisha, India**

# CERTIFICATE

This is to certify that the thesis entitled, "**Effect of Processing, Dopant and Microwave Sintering on the Dielectric Properties of $BiFeO_3$ Ceramic**" being submitted by **Mr**. **Uttam Kumar Chanda,** for the degree of **Master of Technology** in **Ceramic Engineering** to the National Institute of Technology, Rourkela, is a record of bonafide work carried out by him under my supervision and guidance. His thesis, in my opinion, is worthy of consideration for the award of degree of Master of Technology in accordance with the regulations of the institute.

To the best of my knowledge, the matter embodied in the thesis has not been submitted to any other University/ Institute for the award of any degree or diploma.

**Dr. Ranabrata Mazumder**
Associate Professor,
Department of Ceramic Engineering,
National Institute of Technology,
Rourkela

# Contents

# Acknowledgments

This dissertation would not have been possible without the guidance and the help of several individuals who in one way or another contributed and extended their valuable assistance in the preparation and completion of this study.

Foremost, I would like to record my sincere gratitude to **Prof. Ranabrata Mazumder,** for his supervision, patience, motivation and immense knowledge. It was his thought, which both of us tried to achieve. I really learned a lot while working with him during this whole one year.

I am grateful to **Prof. S. K. Pratihar,** Head of Department, Ceramic Engineering, NIT Rourkela for providing me the necessary facilities required during my project work. My sincere thanks to **Prof. J. Bera, Prof. S. K. Pal, Prof. B. B. Nayak, Prof. R. Sarkar** and **Mr. Arun Chowdhury** for their constant help, support, encouragement and blessings which helped to complete my project work.

I am grateful to **Prof Pawan Kumar,** Department of Physics, NIT Rourkela for permitting me to carry out dielectric measurements in his laboratory.

I am very grateful to all the non-teaching members of the department for their help whenever needed in the research work.

I would like to thank all the PhD. and M. Tech (Research) students in our department for their constant help and encouragement. I would like to especially thank **Mr. Ganesh Kumar Sahoo, Mr. Subrat Kumar Mohanty** and **Miss Geetanjali Parida** without whose constant help, support and encouragement, my project work would not been completed. I would like to give thanks to **Miss Prativa Adhikari, Mr. Jayarao Gorinta, Mr. Ezhil Venuswaran** and **Mr. Abhishek Badolia** for their constant help.

I feel guilty if I miss the opportunity to thank my friends; **Gaurav Gugliani, Denny K Philip, Tynee Bhowmick, Subham Mahato, Mandvi Saxena** and **Aditya Prakash Shrimali** who helped me a lot in my research work. I thank all of my friends for their help and support.

I am very grateful to my **PAPA** and **MAA** and my other family members for their faith and support on me, without which I wouldn't have been here to do the work.

Lastly, I owe my deepest gratitude to "**The Almighty God**" & all of them, whose blessings are with me.

Uttam Kumar Chanda

## Abstract

$BiFeO_3$ is of much importance for novel applications as sensors as well as actuators due to the coupling between magnetic and electric domains above room temperature and accepted high polarization in single crystal and thin film. Bulk $BiFeO_3$ suffers from high impurity phase, poor sinterability and high dielectric loss and weak magnetism. The need of the hour is to prepare nanosize $BiFeO_3$ powder with least amount of impurity phase that can be sintered to high density. Doping with suitable ion is required to improve the magnetic property of $BiFeO_3$.

In present work phase pure $BiFeO_3$ is prepared by hydrothermal technique at $200^oC$. KOH concentration in solution controls the phase purity, powder morphology and particle size. Particle size was in the range of 15-20μm. Effect of polyvinyl alcohol as an additive to control the particle size was also studied. $BiFeO_3$ and samarium doped $BiFeO_3$ was also prepared by solid state method using nanosized $Fe_2O_3$ and $Bi_2O_3$. $BiFeO_3$ with lowest impurity content can be prepared above $800^oC$. It is also found that samarium (Sm) doping in $BiFeO_3$ significantly reduces the impurity content, grain size in sintered body and modifies crystal structure. With increase in Sm content, the phase purity was increased from 95% to 99%, upto 10% of Sm doping and then decreases for higher Sm content. The synthesized powder was sintered by conventional sintering and microwave sintering. Microwave sintering significantly reduces firing time but promotes grain growth. Microwave sintered sample has lower dielectric loss compared to conventional sintered $BiFeO_3$.

# List of figures

# List of tables

**Page No**

# Chapter 1

# Introduction

# 1. Introduction

A ferroic crystal contains two or more possible orientation states or domains; under a suitably chosen driving force the domain walls move, switching the crystal from one domain state to another. Switching may be accomplished by mechanical stress ($\sigma$), electric field (E), magnetic field (H), or some combination of the three. Ferroelectric, ferroelastic and ferromagnetic materials are well-known examples of primary ferroic crystals in which the orientation states differ in spontaneous polarization ($P_s$), spontaneous strain ($x_s$) and spontaneous magnetization ($M_s$), respectively. It is not necessary, however, that the orientation states differ in the primary quantities (strain, polarization, or magnetization) for the appropriate field to develop a driving force between orientations. If, for example, the presence of twins between domains leads to a different orientation of the compliance tensor, a suitably oriented stress can produce different strains in the two domains. The stress may act upon the difference in induced strain to produce wall motion and domain reorientation. Aizu **[1]** suggested the term ferrobielastic to distinguish this type of response and illustrated the effect with Dauphine twinning in quartz. Other types of secondary ferroic crystals are listed in Table 1.1, along with the difference between the domain states, and the driving field required to switch between states **[2]**.

Fig.1.1 represents the relationship among different electrically polarizable and magnetically polarizable materials **[3]**. There are a large number of electrically and magnetically polarizable materials, but only few exhibits ferroelectric and ferromagnetic ordering. Materials which are electrically and magnetically polarizable at the same time are referred as magnetoelectric materials. The multiferroic material should have more than one primary ferroic properties.

Now in broader sense multiferroics defined as, at least, two of the three orders or degrees of freedom- (anti)ferromagnetic, (anti)ferroelectric, and ferroelastic—coexisting. The coupling among them, are rare in nature as transition metal ions with active *d* electrons often tend to reduce the off-center distortion necessary for ferroelectricity **[4]**.

**Table 1.1**: Primary and Secondary ferrroics

| **Ferroic class** | **Orientation state differ in** | **Switching force** | **Example** |
|---|---|---|---|
| **Primary** | | | |
| Ferroelectric | Spontaneous polarization | Electric field | $BaTiO_3$ |
| Ferroelastic | Spontaneous strain | Mechanical stress | $CaAl_2Si_2O_8$ |
| Ferromagnetic | Spontaneous magnetization | Magnetic field | $Fe_3O_4$ |
| **Secondary** | | | |
| Ferrobielectric | Dielectric Succeptibility | Electric field | $SrTiO_3$ (?) |
| Ferrobimagnetic | Magnetic Succeptibility | Magnetic field | NiO |
| Ferrobielastic | Elastic compliance | Mechanical stress | $SiO_2$ |
| Ferroelastoelectric | Piezoelectric coefficient | Electric field and mechanical stress | $NH_4Cl$ |
| Ferromagnetoealstic | Piezomagnetic coefficient | Magnetic field and mechanical stress | $FeCO_3$ |
| Ferromagnetoelectric | Magnetoelectric coefficient | Magnetic field and electric field | $Cr_2O_3$ |

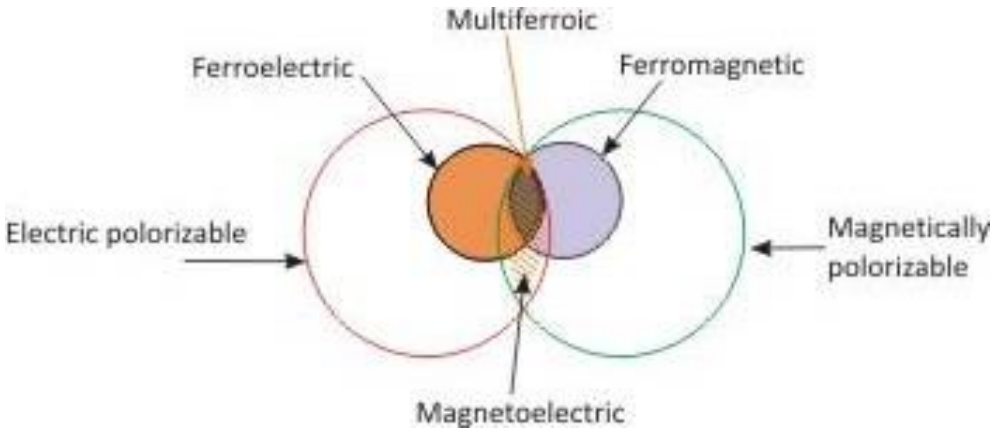


Fig.1.1 The relationship among different electrically polarizable and magnetically polarizable materials

Recently, researches have classified multiferroics into Type I and type II. In Type I multiferroic material, the ferroelectricity and magnetism are originated from different sources and the effects are independent of each other, and a small degree of coupling exists, e.g. Bismuth ferrite ($BiFeO_3$), bismuth manganite ($BiMnO_3$), Yttrium manganite ($YMnO_3$). While in type II material, magnetism causes the existence of ferroelectricity resulting to the strong coupling between two states. Kimura et al. reported that $TbMnO_3$ shows type II multiferroic property by showing the presence of spontaneous polarization in its magnetized state. Other materials showing such effects are also studied namely, $Ni_3V_2O_8$, $MnWO_6$ **[5, 6].**

### 1. 1 Bismutth ferrite ($BiFeO_3$)

Most widely studied multiferroic material is bismuth ferrite. The study of $BiFeO_3$, as a multiferroic material, had been started in 1958 by Smolenskii and colleagues but they were not able to grow single crystals and the polycrystalline ceramics were not useful for practical applications owing to their high conductivity **[7].**

Bismutth ferrite ($BiFeO_3$) has very high ferroelectric curie temperature ($T_C$=1100K or 827°C) and shows G-type antiferromagnetism having cycloidal spin structure with Neel temperature ($T_N$=650K or 377°C). In its ferroelectric state, $BiFeO_3$ shows a rhombohedrally distorted

pervoskite structure (space group R3c) having lattice parameters, $a_r$=3.965 Å and $\alpha_r$=89.4° at room temperature (Fig.1.2) [3]. This G- type antiferromagnetism in $BiFeO_3$ is mainly because in BFO each $Fe^{3+}$ with spin up is surrounded by six of the nearest Fe neighbors with spin down. The spins are not perfectly antiparallel. A weak canting moment is exist. The net magnetic moment (shown in Fig.1.3) arises from canted antiferromagnetic spin has long range superstructure consisting of a spin cycloid with a long repeat distance of 62-64 nm **[3, 8].**

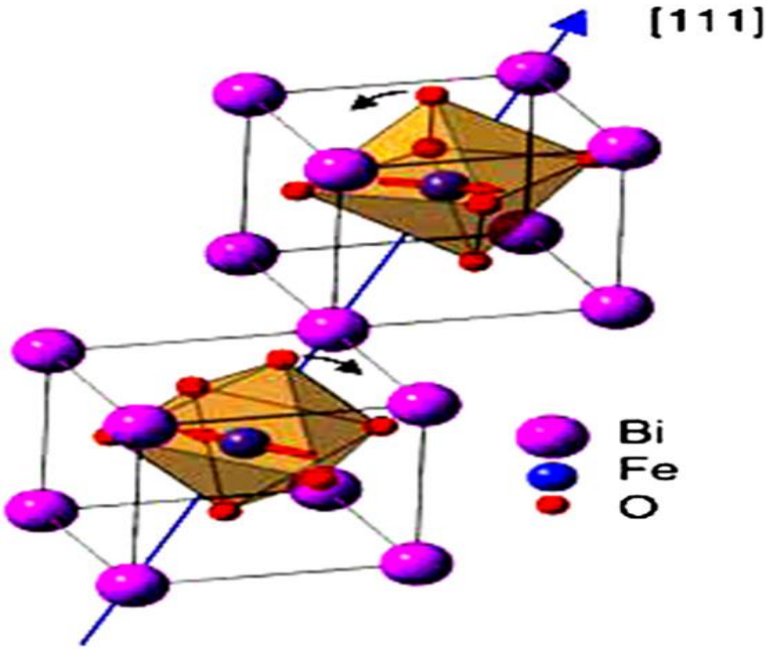


Fig.1.2 Schematic view of the *R*3*c* symmetry built up from two cubic perovskite unit cells

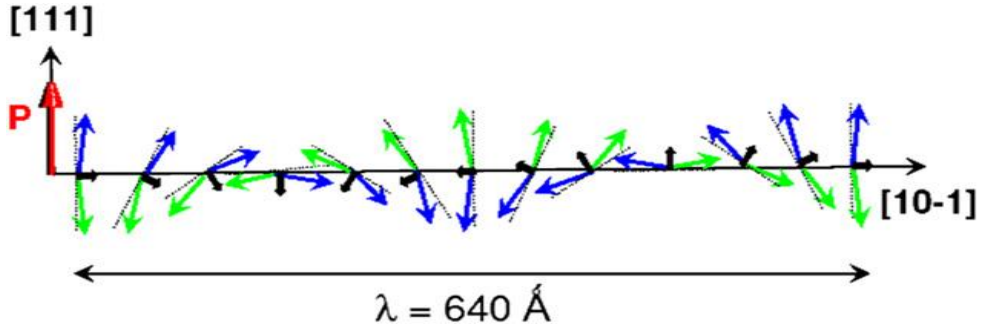


Fig.1.3 Schematic representation of $BiFeO_3$ spin structure **[8]**

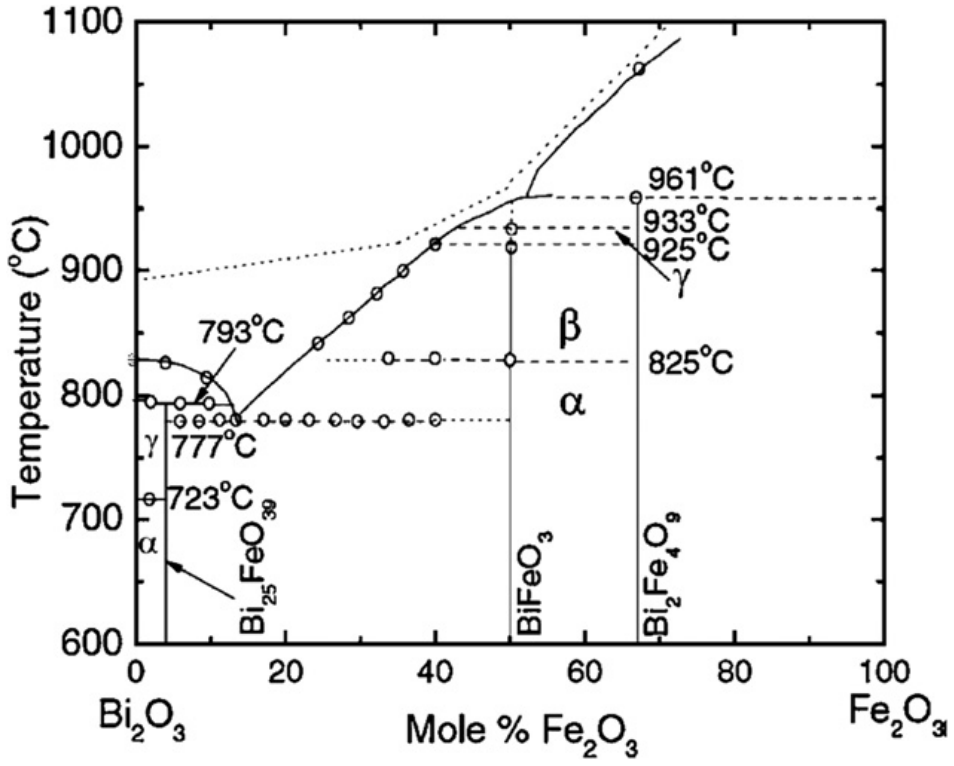


Fig.1.4 Phase diagram of Bismuth ferrite ($BiFeO_3$) **[3]**

$BiFeO_3$ is formed at 50:50 molar ratio of $Bi_2O_3$ and $Fe_2O_3$. With increase in temperature above 825°C, it undergoes structural phase transition to an orthorhombic β-phase and above 931°C; it changes to cubic γ-phase **[3].** It has been told that $BiFeO_3$ is in fact metastable in air, and very prone to show parasitic phases ($Bi_{25}FeO_{39}$ and $Bi_2Fe_4O_9$) that tend to nucleate at grain boundaries well below the melting temperature.

$BiFeO_3$ is ferroelectric at room temperature with high remanent polarization, more than 50 $\mu C/cm^2$ in both of its single crystal and thin film form **[9, 10].** However depending upon the methods of preparation, polycrystalline thin films can be leaky **[3].** On the other hand, pure phase in single crystal form is antiferromagnetic, there have been controversies on magnetism of thin films. Often, impurities like $Fe^{2+}$ and different iron borne impurities as well as deoxygenation can result in significant magnetism **[3].** Fujino et al. **[11]** showed that in samarium modified $BiFeO_3$ ($Bi_{0.86}Sm_{0.14}FeO_3$) morphotropic phase boundary exist and out-of-plane piezoelectric coefficient comparable to those of epitaxial (001) oriented $PbZr_{0.52}Ti_{0.48}O_3$ (PZT) thin films at

the MPB. The composition may be a strong candidate of a Pb-free piezoelectric replacement of PZT.

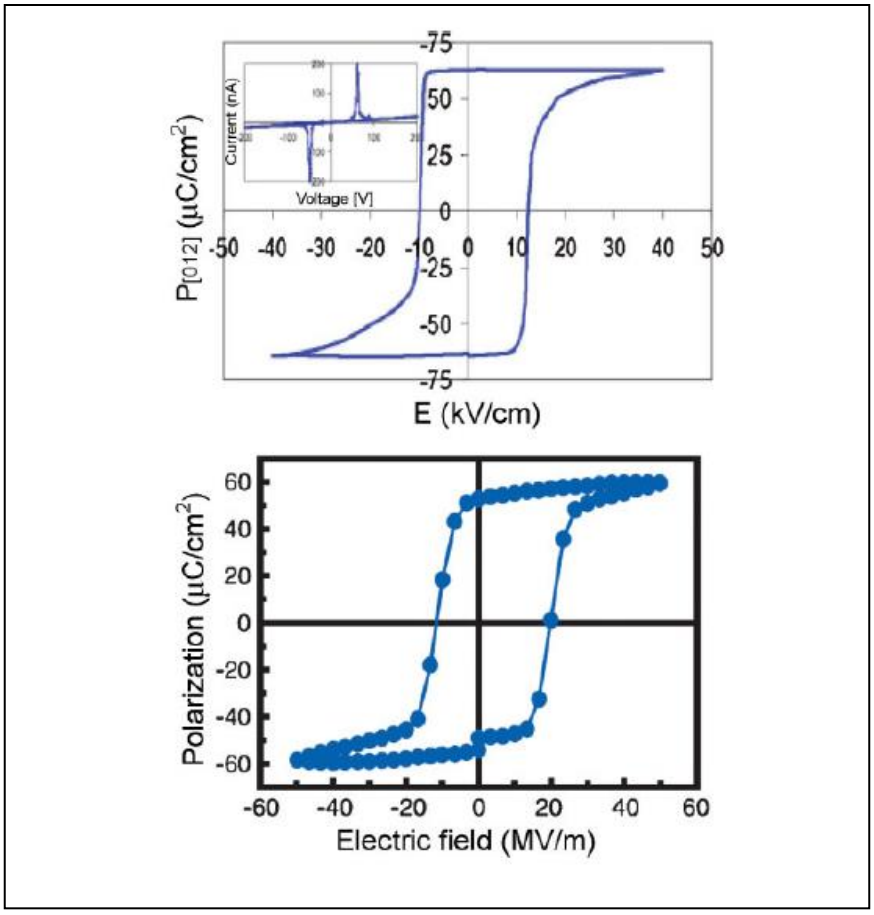


Fig.1.5 Polarization of $BiFeO_3$ (a) bulk single crystal (b) Thin film **[9, 10]**

Although promising for its multiferroic character, only poor dielectric and ferroelectric properties (low values of the polarization and of the dielectric constant) were found at room temperature in the bulk ceramics, mainly due to the semiconducting character which does not allow proper electrical poling and leads to high dielectric losses.

## 1.2 Application of $BiFeO_3$:

Due to its very high polarization in thin film form it is an important candidate for ferroelectric memory application. By forming solid solution with other ferroelectric compound it could be a promising lead free piezoelectric. Due to the observation of orders of magnitude large magnetoelectric coupling and the application potential of these systems in a range of devices

based on “spintronics,” magnetoelectric sensors, electrically driven magnetic data storage and recording devices, magnetocapacitive devices, nonvolatile memories, etc **[3, 12]**.

## Reference


1. K. Aizu, J. Phys. Soc. Japan., 34, 121 (1973).
2. R.E.Newnham, Structure-Property Relations, Springer-Verlag, p. 95 (1975).
3. Eerenstein, W., Mathur, N. D and Scott, J. F., *Nature*, 2005, 442, 759-765, (2006)
4. H. Schmid, Ferroelectrics 162, 317 (1994).
5. NPTEL lecture, Multiferroic and Magnetoelectric Ceramics.
6. T. Kimura1, T. Goto, H. Shintani, K. Ishizaka, T. Arima and Y. Tokura, Nature, 426, p55, (2003).
7. Smolensky GA, Isupov VA, Agronovskaya AI. Sov Phys Solid State;1,15-11, 959
8. D. Lebeugle, D. Colson, A. Forget, M. Viret, A. M. Bataille, A. Gukasov, Phys. Rev. Lett. 2008, 100, 227602.
9. D. Lebeugle, D. Colson, A. Forget, M. Viret, P. Bonville, J. F. Marucco, and S. Fusil, Phys. Rev. B 76, 024116 (2007).
10. J. Wang, J. B. Neaton, H. Zheng, V. Nagarajan, S. B. Ogale, B. Liu, D. Viehland, V. Vaithyanathan, D. G. Schlom, U. V. Waghmare, N. A. Spaldin, K. M. Rabe, M. Wuttig, and R. Ramesh, Science 299, 1719 (2003).
11. S. Fujino, M. Murakami, V. Anbusathaiah, S.-H. Lim, V. Nagarajan, C. J. Fennie, M. Wuttig, L. Salamanca-Riba, I. Takeuchi, Appl. Phys. Lett. 2008, 92, 202904.
12. M. Fiebig, J. Phys. D 38, R123, 2005.

# Chapter 2

# Literature Review

# 2. Literature Review

Perovskite bismuth ferrite being multiferroic is used widely in ferroelectric memory devices, piezoelectric sensors, spintronics; etc [**1**]

## 2.1 Synthesis of Bismuth Ferrite:

Due to the wide range of applications, bismuth ferrite has been synthesized using different methods to obtain BFO micrometer- and nanometer- sized crystallites.

### 2.1.1 Solid State technique:

Solid state synthesis is one of the most widely used and useful method of preparation of BFO. . Progress in solid state synthesis route is mainly because of the demands of industry, and purely academic curiosity. Solid state synthesis of BFO have been reported in many works till now. Synthesis of $BiFeO_3$ by solid state was first carried out by Filipev *et al* [**2**] in 1960. Later, Achenbach *et al* [**3**] also tried to synthesize phase pure $BiFeO_3$ by solid state synthesis. Even they had tried several variation in sintering temperature, time and atmosphere, they failed to synthesize phase pure $BiFeO_3$ due to the presence of secondary phase $Bi_2O_3$ and $Bi_2Fe_4O_9$. To overcome this problems, they synthesized $BiFeO_3$ with excess $Bi_2O_3$, which removed by leaching with concentrated $HNO_3$.

Achenbach *et al* [**4**], also studied BiFeO3 synthesis by solid state method by taking stoichiometric amount of bismuth(III) oxide [$Bi_2O_3$] and iron(III) oxide or ferric oxide [$Fe_2O_3$] are mixed properly and reacted at temperature range of 800°-830°C and removal of unreacted $Bi_2O_3$/$Bi_2Fe_4O_9$ is carried out by washing in $HNO_3$. The main disadvantage of this process is the leaching of the unwanted phases using an acid and subsequently providing coarser powder. Also it is observed that most of the high temperature operation (>800°C) results in bismuth volatilization.

Valant *et al* [**5**], synthesized $BiFeO_3$ using solid state route. Stoichiometric amount of $Bi_2O_3$ and $Fe_2O_3$ are taken. For some experiments, 0.1 and 0.5 wt % of $SiO_2$, $TiO_2$ and $Al_2O_3$ were deliberately added. These powders are mixed properly followed by reacting at 800°C for 5 hours.

The reacted mixtures are then milled, pressed followed by sintering at 880°C for 02-05 hours. By studying phase analysis, Valant *et al* suggested that the synthesis of phase pure polycrystalline BFO can be achieved successfully depending on the purity of starting material. The impurity present in the starting material forces the $Bi_2O_3$ - $Fe_2O_3$ system to form sillenite phase such as $Bi_{25}FeO_{39}$. The sillenite phase further results in increase in fraction of $Bi_2Fe_4O_9$ phase. Though ultrapure starting material are too expensive, the formation of unwanted phase can be reduced by a small $Bi_2O_3$.

Bernardo *et al* [**6**] describes reaction mechanism in synthesis of single phase multiferroic $BiFeO_3$ using solid state synthesis. In the reported work, stoichiometric amount of $Bi_2O_3$ and $Fe_2O_3$ were weighed and milled for 2 hours using ethanol as liquid medium. The milled powder is then dried followed by pressing to make pellet. Firstly, firstly firing was carried out at a temperature range from 600°-1000°C, with soaking time of 02-48 hours. In addition to this, pellets and powders were tested in fast firing treatments, where pellets and powders were introduced carefully inside a pre-heated furnace, dwelled for specific time and rapidly quenched in liquid nitrogen. The soaking times and temperature remain the same in both the methods. Bernardo *et al* further prepared BFO samples using co-precipitation method, where stoichiometric amount of $[Bi(NO_3)_3.5\,H_2O]$ and $[Fe(NO_3)_3.9\,H_2O]$ were dissolved in $HNO_3$ solution. The above solution is then added drop wise into $NH_4OH$. The resultant precipitate is then filtered, washed several times. The powder obtained is then calcined at 300°C. The calcined powder is then milled for 02 hours and the same heat treatment (slow and fast firing) were applied to the powder and pellets. Futhermore, the solid state reactivity of $Bi_2O_3$ - $Fe_2O_3$ system was studied by couples diffusion technique. In co-precipitation method, the secondary $Bi_2Fe_4O_9$ phase was relatively high as compared to solid state method. EDX spectra reveals that the large amount of Bi penetrates several micron inside the $Fe_2O_3$ pellet, and only traces of Fe was found inside the $Bi_2O_3$ pellet. It implies that diffusion of Bi ions activates much before the diffusion of Fe ions. The phase purity of $BiFeO_3$ depends on the diffusion of Bi into the $Fe_2O_3$ grains.

**Reaction mechanism in the solid state synthesis of $BiFeO_3$ [6]:**

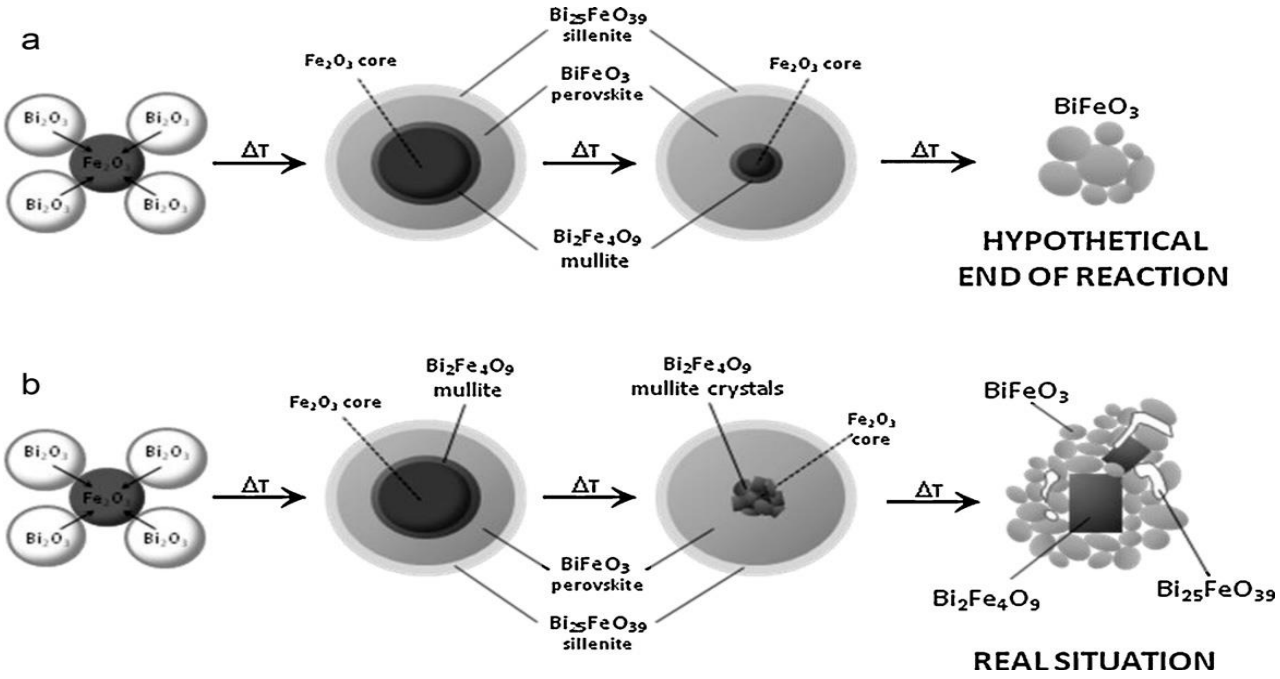


Fig 2.1: Schematic diagram to show the reaction mechanism in solid state synthesis of $BiFeO_3$

a) Hypothetical end of reaction b) Real situation

The diffusion of $Bi^{3+}$ ions into $Fe_2O_3$ is mainly responsible for the formation of pure pervoskite bismuth ferrite in solid state synthesis, where secondary phases are also generated. Initially in the shell, sillenite-type phase ($Bi_{25}FeO_{39}$) is formed whereas in the $Fe_2O_3$ core where the reaction/diffusion takes place, mullite phase ($Bi_2Fe_4O_9$) is generated. In between the core and the shell, pervoskite $BiFeO_3$ forms as the diffusion proceeds. In hypothetical end of reaction, the secondary sillinete and mullite phases should decompose entirely to form single phase pervoskite $BiFeO_3$. But in real situation, with increase in temperature along with the diffusion of Bi ions, crystallization of mullite ($Bi_2Fe_4O_9$) nuclei takes simultaneously. This crystalized mullite particles are highly stable and the resulting in the end of reaction. Thus, along with the $BiFeO_3$ other two phases also coexist in the final product.

### 2.1.2 Wet Chemical Methods:

#### 2.1.2.1. Co-precipitation Method:

Shetty *et al* reported to synthesize BFO using cprecipitation method, in which stoichiometric amount of $Bi_2O_3$ and $Fe_2O_3$ powders are mixed together in nitric acid and diluted with deionized water, ammonia is used to precipitate both the cations (Bi and Fe). The precipitate was washed with de ionized till the pH of the filtrate decreases to 7. It is then dried and then calcined at 500°C for 1 hour, followed by sintering at 810°C for 1 hour [**7].**

#### 2.1.2.2. Ferrioxalate precursor method:

Ghosh *et al* [**8**] had reported 90% phase pure $BiFeO_3$ can be obtained by ferrioxalate precursor method where metal ions to oxalic acid ratio is ~ 0.5, calcination is done at 600°C for 2 hours.

#### 2.1.2.3. Mechanochemical method:

Szafraniak *et al*. [**9**] synthesized bismuth ferrite nanopowder by mechanochemical synthesis, where stoichiometric amount of $Bi_2O_3$ and $Fe_2O_3$ powders are milled for different periods between 05 to 120 hours at room temperature.

#### 2.1.2.4. Solution combustion synthesis process:

Mazumder *et al.* had reported that nanosized BFO can also be prepared by glycine combustion synthesis process. In this method, phase pure $BiFeO_3$ can be prepared by maintaining glycine to nitrate ratio at 0.1. In nanosized powder (4-40nm), saturation magnetization of ~0.4$\mu_B$/Fe along with room temperature ferroelectric hysteresis loop was observed, however in bulk form BiFeO3 exhibit weak magnetization (~0.02 $\mu_B$/Fe) and an antiferromagnetic order [**10**]. In glycine containing system [**11**], few amounts of secondary phases (such as $Bi_2Fe_4O_9$ and $Bi_{36}Fe_2O_{57}$) are also found along with $BiFeO_3$ as major phase, after annealing at 650°C. Paraschiv *et al* [**11**] reported synthesis of $BiFeO_3$ by using urea or glycine as fuel. While by using glycine as fuel, additional secondary phases ($Bi_2Fe_4O_9$ and $Bi_{36}Fe_2O_{57}$) are found, but by using urea as the fuel only few traces of $Bi_2Fe_4O_9$ are observed along with BFO particles of uniform particle shape and size. In wet chemical method [**12**], 0.2 M bismuth nitrate [$Bi(NO_3)_3 5\ H_2O$] and 0.2 M iron nitrate [$Fe(NO_3)_3 9\ H_2O$] are weighed in stoichiometric amount, respectively.. Then 10 g of citric acid

($C_6H_8O_7$) are added to the solutions as chelating agent. The solution is then heated until gel formation takes place. The solid deposits are then kept inside the oven at 150°C for 23 hours. The powders are calcined at different temperature ranging from 350°C to 550°C for 2 hours. It had also been reported to prepare BFO by same technique by using tartaric acid as chelating agent [**13**].

#### 2.1.2.5. Sol-gel technique:

Kumar *et al* observed that single phase $BiFeO_3$ (~200mn) can be synthesized by Sol–gel technique [**14**], followed by leaching. It has been noted that annealing under Argon atmosphere results in decrease in secondary phases but created large oxygen vacancies, subsequently the composition changes to $BiFeO_{2.75}$ rather than $BiFeO_3$

#### 2.1.2.6. Microwave assisted hydrothermal technique:

Biasotto *et al* [**15**] described synthesis of $BiFeO_3$ using microwave assisted hydrothermal method in the temperature of 180°C with soaking varying from 5 min to 1 hour. With increase in soaking time, the impurity phase formation is refrained and resulting in the formation of almost single phase $BiFeO_3$ with homogeneous size distribution of sub-micron $BiFeO_3$ powders.

#### 2.1.2.7. Micro-emulsion technique:

Das *et al* [**16**] explains the single phase nano-sized $BiFeO_3$ can be prepared by micro-emulsion method in the temperature range from 400°C and 500°C. It has been observed that using micro-emulsion technique, better particle size, surface area and sintered density can be achieved.

#### 2.1.2.8. Hydrothermal technique:

The first report of the hydrothermal growth of crystals [**17**] was made by German geologist Karl Emil von Schafhäutl (1803-1890) in 1845. He grew microscopic quartz crystals inside a pressure cooker. Now a days hydrothermal technique is being utilized in synthesis of structural ceramics as well as electronic ceramics.

Chen *et al* observed that large scale growth of BFO particles can be made by using hydrothermal synthesis [**18**]. Here, stoichiometric amount of bismuth nitrate [$Bi(NO_3)_3 5\ H_2O$] and ferric nitrate

[$Fe(NO_3)_3 9\,H_2O$] were dissolved in distilled water, followed by slowly addition of KOH solution to the above solution. A brown suspension is observed which is then transferred into Teflon coated autoclave were reaction is carried out at 200°C for different temperatures (30min, 03hrs, 06hrs, 12hrs and 24 hours). The heating and cooling rates were designed as 2°C/min and 0.2°C/min, respectively. After cooling down to room temperature, the product is washed several times and then oven dried at 70°C. Phase pure $BiFeO_3$ is formed when the KOH conc. are in the range of 1-9M. Chen *et al* [**18**] had observed that the concentration of KOH (01- 10 M), reaction time, the rate of heating and cooling had several impact on the size and morphology of $BiFeO_3$ particles. It has been reported that $Bi_2Fe_4O_9$ and $Fe_2O_3$ phases appeared at KOH concentration 10M, while $Bi_{25}FeO_{39}$ appeared at concentration less than 1M. It has also been reported that unwanted phase $Bi_2Fe_4O_9$ and $Fe_2O_3$ appeared at reaction time of about 30 min. But with increase in the reaction time pure phase $BiFeO_3$ appeared. Chen et al also explained the mechanism of formation of $BiFeO_3$ at higher temperature.

**Stages involved in formation of $BiFeO_3$ using hydrothermal technique [18]:**

1. Transformation of nitrates to hydroxide precipitate after addition of KOH:
   $Bi(NO_3)_3 + Fe(NO_3)_3 + 6KOH \longrightarrow Bi(OH)_3 + Fe(OH)_3 + 6KNO_3$

2. Hydroxide precipitates reacts to form $Bi_2Fe_4O_9$ and $Fe_2O_3$ under hydrothermal environment:
   $25\ Bi(OH)_3 + 3Fe(OH)_3 \longrightarrow Bi_{25}FeO_{39} + Fe_2O_3 + 42\ H_2O$

3. Reaction of mixture in the hydrothermal condition with high temperature and pressure to form $BiFeO_3$:
   $Bi(OH)_3 + Fe(OH)_3 \longrightarrow BiFeO_3 + 3H_2O$
   $Bi_{25}FeO_{39} + 12\ Fe_2O_3 \longrightarrow 25\ BiFeO_3$

With the increase in reaction time, the particle morphology changes from spherical agglomeration to polyhedron [**18**]. Spherical agglomeration occurred for short reaction time of 3

hours, some polyhedrons appear at 6 hours reaction time, truncated octahedrons for 12 hours and final cubo-octahedron for 24 hours in SEM figures.

**Growth mechanism in hydrothermal technique:**

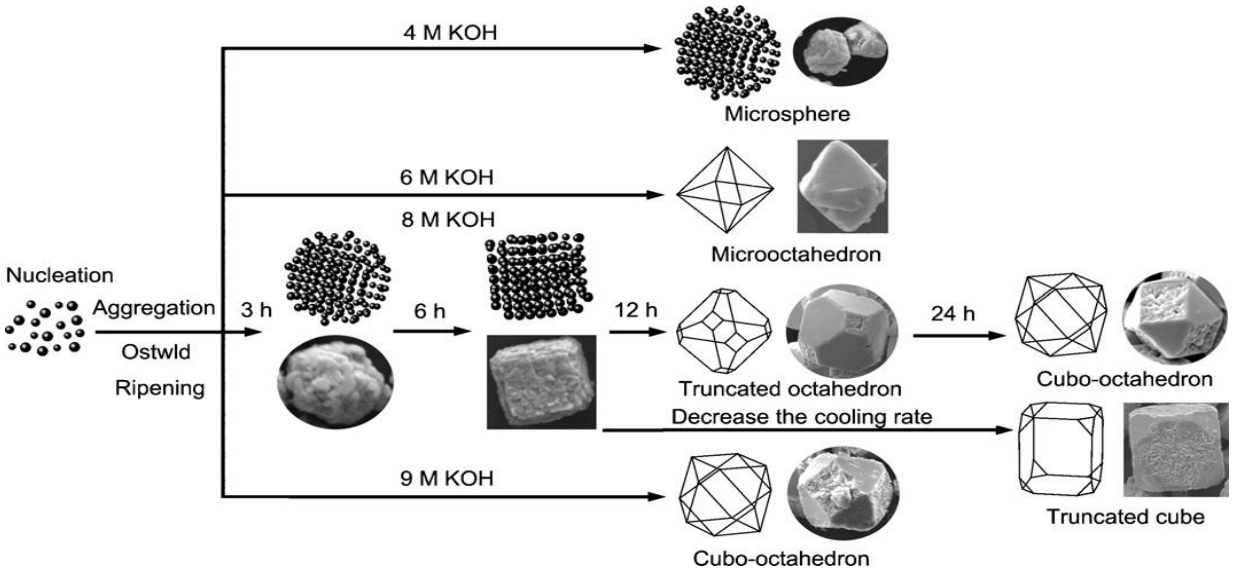


Fig 2.2: Schematic illustration of the growth mechanism and the shape-evolution process of $BiFeO_3$ crystals [**18**]

In the nucleus formation stage, the solute concentration reaches the critical supersaturation stage to nucleate. In hydrothermal environment, nucleation and growth of small crystallites simultaneously takes place, resulting in a lot of $BiFeO_3$ nanoparticles formation and agglomeration.

1. At low KOH concentration, surface energy don't change & the nanoparticles agglomerate to isotropic spheres.
2. With increasing KOH concentration, the particle size increases from 10 μM to 20 μM approximately & the morphology changes from irregular agglomeration to regular polyhedron.
3. At 6M KOH concentration, $BiFeO_3$ particles become homogeneous octahedron of about 8μM.

4. At high KOH concentration, KOH could change the surface energy of the particle & an oriented attachment process dominates results in the octahedron shape.

In hydrothermal condition, the surface of bismuth ferrite particle is negatively charged [19]. Different KOH concentrations can result in different distribution of surface charge of the nanoparticles, which lead to the selective aggregation occurrence to form different polyhedrons.

Zhang *et al* [**20**], reported that too high alkali concentration decreases the crystallinity of BFO powders. The particle size increases with the increasing hydrothermal temperature but it was lower than that with the increasing alkali concentration Phase pure BFO can be syntheized when the KOH concentration was 8 mol/L. When the molar ratio of $Bi^{3+}$ to $Fe^{3+}$ ions was controlled in the range from 9:10 to 10:10, no secondary phases such as $Bi_2Fe_4O_9$ or $Bi_{25}FeO_{40}$ formation takes place. The BFO powders exhibit the remanent magnetization of 0.011 emu/g and the coercive field of 219.2 Oe when its particle size decreases to 56 nm. The Neel temperature decreases from 378.21 to 365.81°C with the decreasing average particle size of BFO powders. The decrease in $T_N$ of BFO powders could be related to the decrease in spontaneous polarization and the number of antiferromagnetic interactions with the decreasing particle size.

Han *et al* [**21**] observed that with increasing KOH concentration, the particles became smaller and their morphology changed from plate to spherical like, and they were more agglomerated. With the high KOH concentration results in a high nucleation rate for the BFO phase. This explain the decrease of the particle size with increasing KOH concentration. The optimum conditions to retain pure-phase BFO were determined to be a KOH concentration of 8 M for a reaction time of 6 h at 175–225°C. BFO particle growth was promoted by lowering the KOH concentration, or increasing duration time or reaction temperature.

It has also been reported [**22**] that the BFO powders, prepared without $KNO_3$, consist of uniform rectangle crystallites with a side length of about 250 nm and a thickness of about 100 nm. But when the mineralizer $KNO_3$ was introduced into the process, uniform spherical BFO particles about 5 nm in size are formed. The main reason reported for the above process is that the dissolution of $NO^{3-}$ ions in the supersaturated hydrothermal fluid noticeably decreased the

growth speed of BFO nuclei and facilitated a faster nucleation of BFO, which finally result in BFO nanoparticles of 5 nm. The improved magnetism of the BFO crystallites at room temperature can be achieved with the decrease to a nanometer scale in particle size.

Hojamberdiev *et al* [**23**] studied the control of morphology of bismuth-ferrite using various alkaline mineralizers (KOH, NaOH, LiOH). It has been reported that the secondary phase $Bi_{25}FeO_{40}$ and $Bi_2Fe_4O_9$ are formed when the concentration of alkaline solutions were either high or low. BFO powders have laminar with irregular shape, rectangle and rod-like crystallites in the range of nano and sub micrometer due to the influence of KOH, NaOH and LiOH, respectively. It had been reported that with decrease in particle size of bismuth ferrite powders, the magnetic properties improve. Several work have been reported where bismuth ferrite had been prepared by using different additives (or surfactants).

#### 2.1.2.9. Polymer assisted hydrothermal technique:

Wang *et al* [**24**] synthesized BFO nanopowders by polymer assisted hydrothermal route. They used PVA [poly(vinyl alcohol)] as an additive. Bismuth nitrate and ferric nitrate are mixed together followed by addition of the solution to 12M KOH solution. Filtration had been carried out to remove $NO_3^{-1}$ and $K^+$ ions, which is then mixed 30 ml KOH solutions (12M) and 15 ml PVA (4 g/l). The solution is then transferred to an autoclave, the autoclave was sealed and maintained at 160 °C for 9 h, respectively. The products were filtered, washed several times and then dried at 70°C. It has been summarized that the introduction of polymer in hydrothermal process has no effect on the crystallization of BFO crystallites. TEM results shows that without an addition of polymer, BFO crystals were nearly like cubic sugar, with an average side size of about 100–120 nm. But well-crystallized BFO nanoparticles, with an average diameter of about 10 nm formed when PVA was added.

Meher *et al* [**25**], had described the polymer assisted hydrothermal technique for preparation of $CeO_2$ nanoparticle. We tried to synthesize $BiFeO_3$ nanoparticle, keeping in mind the mechanism behind confinement of particle size. It has been noted that as polymer (or surfactant) has been added, the selective adhesion mechanism takes place. This implies that in polymer assisted

method, the polymer selectively adhere to the surface of the nucleation site which results in decrease in growth rate thus making uniform size particle size generation. But without polymer addition the nucleation and growth mechanism takes place simultaneously, which results in agglomeration and growing of large crystallite size.

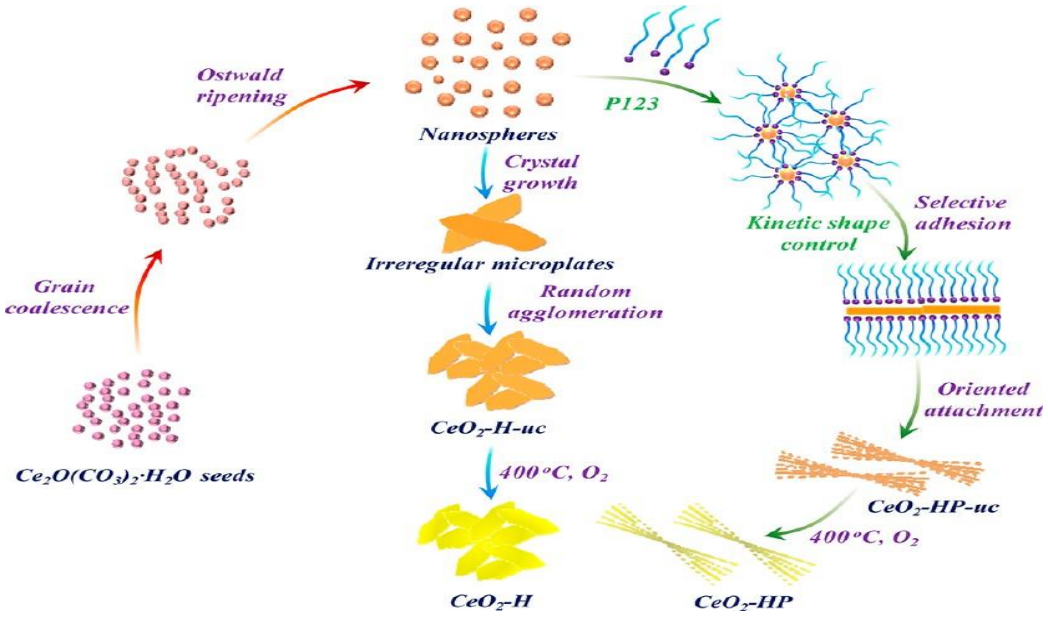


Fig 2.3: Plausible growth mechanism in polymer free and polymer assisted hydrothermal method [**25**].

As it has already been reported that with decrease in particle size, the size confinement effect takes place which result in generation of weak ferromagnetic effect in $BiFeO_3$ at room temperature.

In another work, Cho *et al* [**26**] studied preparation of BFO nanopowders using triethanolamine (TEA) as an additive. It has been observed that in the presence of TEA, pure BFO nanopowders showing spherical morphology with an average size of approximately 100 nm were synthesized at temperatures as low as 130°C. Without TEA some unreacted peaks and intermediate peaks are observed. A relatively large number of Fe ions remain in the solution due to the formation of Fe–TEA complexes and this may reduce the energy required to achieve the BFO phase.

Hydrothermal had several advantages as compared to other techniques such as sol gel, co-precipitation, combustion route, micro-emulsion, etc.

### 2.1.3. Advantages of hydrothermal technique:

1. Single step process.
2. Minimize energy consumption.
3. Closed systems resulting in low environmental impact.
4. Products with much higher homogeneity.

Due to its advantages hydrothermal technique has drawn attention of several scientist as well as technologist.

Table 2.1: Advantages and disadvantage of different wet chemical methods for synthesis $BiFeO_3$ **[16, 27-31]**

| **Synthesis Method** | **Synthesis** | **SD** | **Size range (nm)** | **Shape control** | **Reaction Temperature (°C)** | **Reaction time** | **Reaction yield** | **Annealing temperature (°C)** |
|---|---|---|---|---|---|---|---|---|
| CP | Very simple, ambient condition | Broad/ narrow | 30-100 | Poor | 20-90 | Minutes | High/ Scalable | 550-700 |
| ME | Complicated, ambient condition | Narrow | 15-40 | Good | 20-70 | Hours | Low | 400 |
| HT | Simple, high pressure | Very narrow | >100 | Very good | 150-200 | Hours/ day | Medium | - |
| Sol-gel | Simple | Broad/ narrow | 15-150 | Good | 20-90 | Hours/ day | Medium | 400-600 |
| MHT | Simple, very fast, reproducible | Very narrow | >100 | Good | 100-200 | Minutes | High | - |

**Abbreviations-** SD: Size Distribution; CP: Co-precipitation; ME: Microemulsion; HT: Hydrothermal; MHT: Microwave assisted hydrothermal

## 2.2. Sintering:

As it has already known, that more than 90% theoretical density in $BiFeO_3$ sintered body is difficult to achieve. With increase in porosity permittivity of the material decreases, which ultimately hampers the electrical property of $BiFeO_3$ ceramic. To increase the density of sintered body, several attempts has been made by using different sintering technique.

### 2.2.1. Rapid liquid phase Sintering:

Wang *et al* [**32**] reported that by rapid liquid phase sintering, $BiFeO_3$ has been prepared with 92% relative density, resulting in spontaneous and remanent polarization of about 8.9 and 4.0 $\mu C/cm^2$, respectively. Pradhan *et al* [**33**] also followed same technique, but they haven't reported the densification details. Though they reported the spontaneous and remanent polarization were about 3.5 and 2.5 $\mu C/cm^2$, respectively. Yung *et al* [**34**] synthesized $BiFeO_3$ using rapid liquid phase sintering (855 °C for 5 min at 100 °C/s) having electrical resistivity as high as ~5×1012 Ω cm, relative density ~ 92%. It is also reported that the sample have large saturation polarization of 16.6 $\mu C/cm^2$ and a low leakage current density of 30 $mA/m^2$

### 2.2.2. Spark plasma sintering:

Mazumder *et al* [**35**] reported that dense $BiFeO_3$ ceramic can be prepared by novel spark plasma sintering technique (SPS) at a temperature ranging from 675 to 750°C under 70 MPa pressure. It is observed that 96% relative density is achieved in this method, where as in conventional sintering only 90% of theoretical density is achieved at temperature of about 820°C. But it is observed that at higher temperature, unwanted $Bi_2Fe_4O_9$ phase is generated.

### 2.2.3. Microwave sintering:

Microwave sintering had been emerged in recent years as new sintering technique and shown major advantages against conventional sintering [**36**]. Microwave energy is a type of electromagnetic energy with frequency ranging from 300MHz to 300GHz. Microwave heating is a technique in which material absorb the electromagnetic energy and transform into heat. In conventional heating, heat transfer takes place by conduction, convection and radiation. The material's surface is heated first followed by movement of heat inside the body. Whereas in

microwave sintering, heat is generated inside the body first and then the entire volume gets heated [**37**].

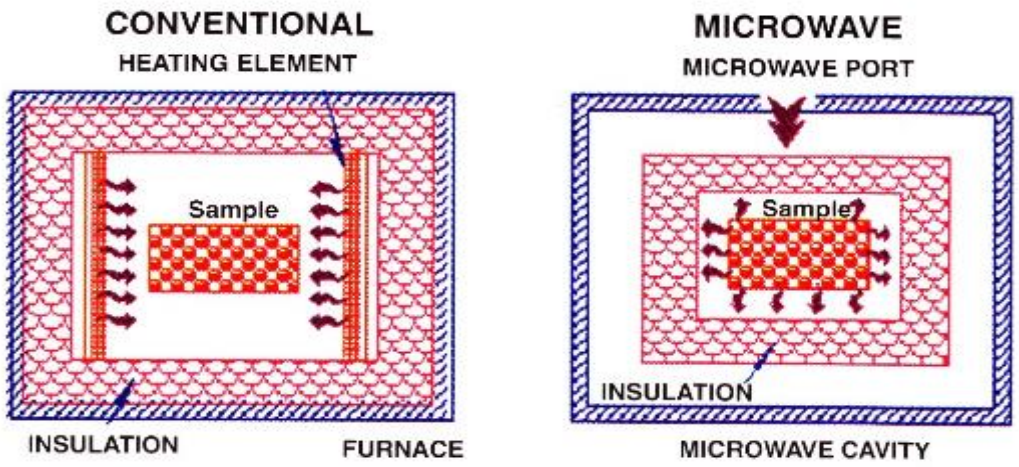


a. Conventional Sintering b. Microwave Sintering

Fig 2.4: Comparison of heating procedure between a) Conventional Sintering b) Microwave Sintering [**38**]

**Interaction of microwaves with materials [39]:**

Materials can be classified into 03 different groups according to the interaction of microwaves with them.

1. **Transparent**: These low dielectric loss materials passes microwave without any losses.
2. **Opaque (Conductor)**: In these materials, microwaves are reflected and don't penetrate.
3. **Absorbing:** These materials are high loss materials, where microwaves are absorbed based on the dielectric loss factor.

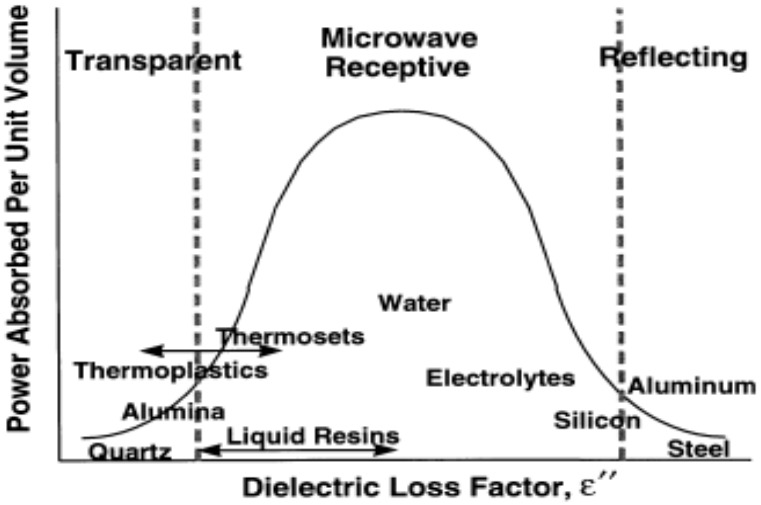


Fig 2.5: Graphical representation of change in power absorbed by materials with respect to dielectric loss factor [**37**]

**Advantages of microwave sintering over conventional sintering** [**37, 39**]**:**

1. It enhances diffusion processes.
2. It reduces energy consumption.
3. It decreases sintering temperature.
4. It reduces processing time as it has very rapid heating and cooling rates.
5. It has low environmental hazards.

Recently Cai *et al* [**39**], had studied the effects of microwave sintering power on properties of $BiFeO_3$ ceramics. It has been reported that single phase $BiFeO_3$ ceramics with high density and uniform grain size can be obtained when BiFeO3 is sintered at 3.4kW. Decrease in dielectric loss is observed when BFO is sintered in lower sintering power. The coercive electric field and remnant polarization decreases with increase in microwave sintering power. The leakage current of $BiFeO_3$ increases with increase in microwave sintering power. Also it has been reported that the coercive magnetic field and the remnant magnetization of microwave sintered $BiFO_3$ increases with increase in microwave sintering power.

Prasad *et al* [**40**] had compared the electrical and magnetic properties of $BiFeO_3$ prepared by solid state route followed by microwave sintered sample with that of the conventionally sintered

samples. It had been observed that microwave sintering results in formation of nano-crystalline samples, whereas by conventional sintering micro-crystalline samples had been obtained, thereby making microwave sintered sample slightly ferromagnetic and conventional sintered sample remains antiferromagnetic. In microwave sintered samples, the dielectric constant increases to more than one order. The electric resistivity increases by 6 times and remnant polarization increases by 4-5 times in microwave sintered sample as compared to conventional sintered $BiFeO_3$ sample.

### 2.3. Problems associated with $BiFeO_3$ ceramics:

The major difficulties faced during synthesis of $BiFeO_3$ ceramic are:

1. Achieving phase pure material.
2. Synthesizing sintered densities having more than 90% of theoretical density and
3. Synthesizing highly resistive $BiFeO_3$ ceramics with less leakage current.

The major problem associated with the synthesis of $BiFeO_3$ ceramic is the formation of unwanted secondary phases. Upper or lower calcinations temperatures results higher content of the secondary phases ($Bi_{25}FeO_{39}$ and $Bi_2Fe_4O_9$) [**14**]. Secondary phases appear due to the kinetics of phase formation.

### 2.4. Reasons for impurity formation in $BiFeO_3$ [27]:

1. Evaporation of Bi component occurs at low temperature on the onset of synthesis, which is due to low decomposition temperature of Bi salts. The $Bi_2O_3$ again appears as the impurity phase in final product.
2. In the phase diagram of $Bi_2O_3$ - $Fe_2O_3$, the synthesis zone of single phase $BiFeO_3$ is very narrow, in which two impurity phase $Bi_{25}FeO_{39}$ and $Bi_2Fe_4O_9$ are usually substitution for $BiFeO_3$.
3. In an oxygen deficient atmosphere, the chemical valence of Fe ion changes. The charge defects with respect to $Fe^{2+}$ ions are related to large leakage current in $BiFeO_3$.

## 2.5. Doping of $BiFeO_3$:

Doping methods have been considered to modify $BiFeO_3$, such that samples exhibit the large magnetic moment and produce large magnetoelectrical coupling, Several studies have been carried out in which $BiFeO_3$ are doped with rare earth metal. Thereby suppressing its cyloid spin structure, and improving the ferroelectric properties because of improved phase stability and decrease in impurity phase formation [**41**]. In $BiFeO_3$, small amount of oxygen vacancies and $Fe^{2+}$ ions exits [**42**]. Bismuth ferrite shows p-type conductivity due to the substitution of $Fe^{2+}$ ions in $Fe^{3+}$ positions. When a heterovalent $A^{2+}$ ions with same ionic radius that of $Bi^{3+}$ ions are doped into the A site, they generate oxygen vacancies but doesn't liberate electrons as follows [**42**]:

$$\tfrac{1}{2}(1\text{-}x)\,Bi_2O_3 + x\,AO + \tfrac{1}{2}\,Fe_2O_3 \longrightarrow (Bi_{1-x})^{3+}(A_x)^{2+}(Fe)^{3+}(O_{3-x/2})^{2-}$$

The hole generated can be consumed by the $Fe^{2+}$ ion which is in the $Fe^{3+}$ position, consequently decrease in acceptor doping of $Fe^{3+}$ by $Fe^{2+}$, thereby decrease in conductivity. The magnetic properties of $Bi_{1-x}A_xFeO_3$ are directly related to the ionic radius of the substituting element [**43**]. Increase in ionic radius of A site ion results in appearance of net magnetism due to suppression of the spiral spin structure of BFO. When higher valence ion such as $Ti^{4+}$, $Zr^{4+}$ and $Nb^{5+}$ substitute $Fe^{3+}$, the doping of $Fe^{3+}$ by $Fe^{2+}$ reduces further because the high valence ions are more electronically stable, this results in decrease in conductivity [**44**]. With the substitution of ions for $Fe^{3+}$, the bond angle Fe-O-Fe increases resulting in improvement of magnetic properties because bond angle increment enhances the superexchange interaction between two Fe ions.

Fanggao *et al* [**44**] synthesized $Bi_{1-x}Gd_xFeO_3$ by conventional solid state technique, stoichiometric amount of $Bi_2O_3$, $Fe_2O_3$ and $Gd_2O_3$ are weighed and thoroughly mixed for about 2 hours using isopropyl alcohol as a liquid medium. The powder is then calcined at 650°C for 1 hour. The calcined powder is then grounded again followed by heating at around 810°C for 1 hour. It has been observed that the dielectric loss and dielectric constant decreases with increase in frequency in the ranging from 100 Hz and 1 MHz. For $Bi_{0.95}Gd_{0.5}FeO_3$, the dielectric constant reaches 600, which is six time bigger than that of pure $BiFeO_3$. The substitution of Gd for Bi

helps in removal of impurity phase in $BiFeO_3$. As the $Gd^{3+}$ content increases the lattice constant of *a* and *c* of the unit cell decreases.

Nalwa *et al* [**45**] studied the effect of Samarium doping on the property of $BiFeO_3$ multiferroic. They synthesized Sm- doped BFO by using solid state method. It has been reported that the phase pure undoped BFO can be achieved by calcining at 825°C. Increased amount of secondary phase can be formed with deviation from calcination temperature. While in $Bi_{0.9}Sm_{0.1}FeO_3$, it has been reported that secondary phase doesn't appear on calcining at 800°C and above for 1 hour. Upon heating upto 500°C, the undoped sample shows paramagnetic behavior, whereas in Sm-doped $BiFeO_3$, the ferromagnetic behavior becomes less and shows antiferromagnetic transition at ~370°C. With Sm doping, the remanent polarization also increase but it is accompanied by higher conductivity in doped samples.

Xu *et al* [**46**] studied the synthesis of polycrystalline $Bi_{1-x}Sm_xFeO_3$ thin film in FTO/glass substrate by sol-gel method. They mentioned that with increase in dopant content, gradual phase transition takes place from rhombohedral to pseudo-tetragonal phase. With proper amount of Sm-doping results in decrease in leakage current. But on the other hand, excess Sm can result in lattice inhomogeneity, thereby increasing more defects in the film and resulting increment in leakage current density. The defects in the complexes in $BSFO_{x=0.06}$ results in decrease in dielectric constant, leakage current and remnant polarization. The $BSFO_{x=0.09}$ thin film shows increase in dielectric constant, remnant polarization, remnant magnetization having values of 203–185, 70 $\mu C/cm^2$ and 1.31 $emu/cm^3$, respectively.

Singh *et al* [**47**] prepared polycrystalline Sm-doped (0 to 10%) $BiFeO_3$ thin films by chemical solution deposition method on $Pt/Ti/SiO_2/Si$ substrate. Pure phase Sm-doped $BiFeO_3$ was obtained up to 10 % Sm atoms, Sm-doped thin film show increased electrical properties. Sm-doping also increases coercive field in the film. On Sm doping up to 7.5 %, there was a noticeable decrease in leakage current density ($10^{-4}A/cm^2$) and increase in polarization ($70\mu C/cm^2$). The undoped $BiFeO_3$ shows magnetic moment $0.04\mu_B$/Fe, whereas the doped $BiFeO_3$ shows magnetic moment of 0.3 $\mu_B$/Fe.

Garcia *et al* [**48**] described synthesis of Lanthanum doped $BiFeO_3$ by polymeric precursor method, also known as Pechini method. It has been observed that below 10% Lanthanum doping, the rhombohedral structure of $BiFeO_3$ is maintained by $Bi_{1-x}$ $La_xFeO_3$. At 30% Lanthanum doping, rhombohedral is transformed into orthorhombic. Further addition of dopant results in structural distortion leading to grains in a plate-like morphology. Though the individual particle size is approximately 30nm.

Du *et al* [**49**] had also studied the properties of Lanthanum doped $BiFeO_3$ using hydrothermal method. It has been observed that the lattice parameter increases with increase in La content, though the Fe-O octahedral becomes more distorted It is reported that the morphology of micron-sized particle changes from spherical to octahedral with variation in dopant concentration. The dielectric constant of $Bi_{1-x}La_xFeO_3$ increases with increase in dopant level, and attains maximum value for $Bi_{0.8}La_{0.2}FeO_3$ in both low and high frequency range at room temperature. The magnetic moment increases from 0.264emu/g of $BiFeO_3$ to 0.658emu/g of $Bi_{0.9}La_{0.1}FeO_3$ in a field of 3t at 77K. Because of Lanthanum substitution, both enhancements in ferroelectric and dielectric properties take place due to change in lattice parameters and Fe-O bond lengths.

## References:


1. Gustau Catalan and James F. Scott, Adv. Mater. 2009, 21, 2463–2485.
2. Filipev, V. S.; Smolyaninov, N. P.; Fesenko, E. G.; Belyeav, I. N. Kristallografiya 1960, 5, 958.
3. Achenbach, G. D. J. Am. Ceram. Soc. 1967, 50, 437.
4. Achenbach G., James W. J. , Gerson R., J. Am. Ceram. Soc. 8 (1967) 437.
5. Matjaz Valant, Anna-Karin Axelsson, and Neil Alford; Peculiarities of a Solid-State Synthesis of Multiferroic Polycrystalline BiFeO3, Chem. Mater. 2007, 19, 5431-5436.
6. M.S. Bernardo, T. Jardiel, M. Peiteado, A.C. Caballero, M. Villegas, Reaction pathways in the solid state synthesis of multiferroic $BiFeO_3$; Journal of the European Ceramic Society 31 (2011) 3047–3053.
7. S. Shetty, V.R. Palkar, R. Pinto, Size effect study in magnetoelectric $BiFeO_3$ system, Pramana J. Phys. 58 (5, 6) (2002) 1027–1030.
8. S. Ghosh, S. Dasgupta, A. Sen, H.S. Maiti, Low temperature synthesis of bismuth ferrite nanoparticles by a ferrioxalate precursor method, Mater. Res. Bull. 40 (2005) 2073–2079.
9. Szafraniak I., Polomska M., Hilczer B., Pietraszko A., K˛epi´nski L. Journal of the European Ceramic Society 27 (2007) 4399
10. Mazumder R., Devi P. S., Bhattacharya D., Choudhury P., Sen A., Raja M., Applied Physics Letters 91 (2007) 062510
11. Paraschiv C. , Jurca B., Ianculescu A., Carp O. Journal of Thermal Analysis and Calorimetry, Vol. 94 (2008) 2, 411.
12. YongmingHu, Linfeng Fei, Yiling Zhang, Jikang Yuan, Yu Wang, and Haoshuang Gu, Journal of Nanomaterials Volume 2011 (2011)
13. S. Ghosh, S. Dasgupta, A. Sen, and H. S. Maiti, "Low-temperature synthesis of nanosized bismuth ferrite by soft chemical route," Journal of the American Ceramic Society, vol. 88, no. 5, pp. 1349–1352, 2005.
14. Kumar M., Yadav K.L., Varma G.D. Materials Letters 62 (2008) 1159

15. G. Biasotto, A.Z. Simo˜es, C.R. Foschini, M.A. Zaghete, J.A. Varela, E. Longo. Materials Research Bulletin 46 (2011) 2543–2547.

16. Nandini Das, Ranabrata Majumdar, A. Sen, H.S. Maiti. Materials Letters, Volume 61, Issue 10, April 2007, Pages 2100-2104.

17. K. Byrappa and Masahiro Yoshimura, Handbook of Hydrothermal Technology (Norwich, New York: Noyes Publications, 2001), Chapter 2: History of Hydrothermal Technology.

18. Xian-Zhi Chen, Zhong-Cheng Qiu, Jian-Ping Zhou, Gangqiang Zhu, Xiao-Bing Bian, Peng Liu, Large-scale growth and shape evolution of bismuth ferrite particles with a hydrothermal method, Materials Chemistry and Physics 126 (2011) 560–567.

19. S.K. Lee, G.J. Choi, U.Y. Hwang, K.K. Koo, T.J. Park, Mater. Lett. 57 (2003) 2201.

20. Haibo Zhang and Koji Kajiyoshi, J. Am. Ceram. Soc., 93 [11] 3842–3849 (2010).

21. Seung Ho Han, Kyoung Sun Kim, Ho Gi Kim, Hyeung-Gyu Lee, Hyung-Won Kang, Jeong Seog Kim, Chae Il Cheon. Ceramics International 36 (2010) 1365–1372.

22. Yonggang Wang, Gang Xu, Zhaohui Ren, Xiao Wei, Wenjian Weng, Piyi Du, Ge Shen, and Gaorong Han, J. Am. Ceram. Soc., 90 [8] 2615–2617 (2007)

23. Mirabbos Hojamberdiev, Yunhua Xu, Fazhan Wang, Juan Wang, Wengang Liu, Mingqiong Wang, Morphology-controlled hydrothermal synthesis of bismuth ferrite using various alkaline mineralizers; July 15, 2008.

24. Yonggang Wang, Gang Xu, Zhaohui Ren, Xiao Wei, Wenjian Weng, Piyi Du, Ge Shen, Gaorong Han, Low temperature polymer assisted hydrothermal synthesis of bismuth ferrite nanoparticles; Ceramics International Volume 34, Issue 6, August 2008, Pages 1569–1571.

25. Sumanta Kumar Meher and G. Ranga Rao, Polymer-Assisted Hydrothermal Synthesis of highly reducible Shuttle-Shaped CeO2, ACS Catal. 2012, 2, 2795-2809

26. Chin Moo Cho, Jun Hong Noh, In-Sun Cho, Jae-Sul An, Kug Sun Hong, Jin Young Kim, J. Am. Ceram. Soc., 91 [11] 3753–3755 (2008).

27. R. Safi, H. Shokrollahi, Progress in Solid State Chemistry 40 (2012) 6-15.

28. Ke H, Wanga W, Wanga Y, Xua J, Jia D, Lub Z, J Alloys Compd 2011;509: 2192-7.

29. Gao F, Chen X, Yin K, Dong S, Ren Z, Yuan F, et al. Adv Mater 2007;19: 2889-92.

30. Park TJ, Papaefthymiou GC, Viescas AJ, Moodenbaugh AR, Wong SS. Nano Lett 2007;7:766-72.

31. Prado-Gonjal J, Villafuerte-Castrejo'n ME, Fuentes L, Mora'n E. Mater Res Bull 2009;44:1734-7.

32. Wang Y.P., Zhou L., Zhang M.F., Chen X.Y., Liu J. M., Liu Z.G., Appl. Phys. Lett. 84 (2004),1731

33. Pradhan A.K., Zhang K., Hunter D., Dadson J.B., Loiutts G.B., Bhattacharya P., Katiyar R., Zhang D.J. J., Sellmyer, J. Appl. Phys. 97 (2005) 093903.

34. Yuan G.L., Or S.W., Wang Y.P., Liu Z.G., Liu J.M. Solid State Commun. 138 (2006)76.

35. Mazumder R., Chakravarty D., Bhattacharya D., Sen A. Materials Research Bulletin 44 (2009) 555.

36. P. Yadoji, R. Peelamedu, D. Agrawal, R. Roy, Materials Science and Engineering B 98 (2003) 269–278.

37. D. Agrawal, Journal of Materials Education 19 (1999) 49–58.

38. D. Agarwal, Transactions of the Indian Ceramic Society, Vol. 65(3), July-September, 2006.

39. Ch. Sree Rama Linga Prasad, G. Sreenivasulu, S. Roopas Kiran, M. Balasubramanian, B. S. Murty, J. Nanosci. Nanotechnology. 11, 4097-4102, 2011.

40. Wei Cai, Chunlin Fu, Wenguang Hu, Gang Chen, Xiaoling Deng. Journal of Alloys and Compounds 554 (2013) 64–71.

41. Dutta DP, Jayakumar OD, Tyagi AK, Girija KG, Pillaia CGS, Sharma G. Nano-scale 2010;2:1149-54.

42. Khomchenko VA, Kiselev DA, Kopcewicz M, Maglione M, Shvartsman VV, Borisov P, et al. Magn Mater 2009;321:1692-8.

43. Kumar M, Yadav KL. J Appl Phys 2006;100:074111-4.

44. Chang Fanggao, Song Guilin, Fang Kun, Qin Ping, Zeng Qijun. Journal of rare earths: Vot.24, Spec. Issue, Dee. 2006, p.273.

45. K.S. Nalwa, A. Garg, A. Upadhyaya. Materials Letters 62 (2008) 878–881.

46. Xue Xu, Tan Guoqiang, Ren Huijun, Xia Ao. Ceramics International (2013), http://dx.doi.org/10.1016/j.ceramint.2013.01.042.

47. S. K. Singh, C. V. Tomy, T. Era, M. Itoh, and H. Ishiwara. Journal of Applied Physics 111, 102801 (2012).

48. F. Gonzalez Garcia, C.S. Riccardi, A.Z. Simões. Journal of Alloys and Compounds 501 (2010) 25–2.

49. Yi Du, Zhen Xiang Cheng, Mahboobeh Shahbazi, Edward W. Collings, Shi Xue Dou, Xiao Lin Wang. Journal of Alloys and Compounds 490 (2010) 637–641.

# Chapter 3

# Summary of Literature Review and Objective

## 3.1. Summary of Literature review:

From literature review it can be summarized that

a) $BiFeO_3$ is of much importance for novel applications as sensors as well as actuators due to the coupling between magnetic and electric domains above room temperature and accepted high polarization in single crystal and thin film.
b) Thus far, the incorporation of bismuth ferrite into practical devices has been hindered by other problems too, e.g., low resistivity (high loss) presumably due to defect and non-stoichiometry related issues. Hence, there has been a pressing need to generate high-quality samples.
c) During synthesis of $BiFeO_3$, the kinetics of formation always leads to a mixture of $BiFeO_3$ as a major phase along with other impurity phases. The task becomes difficult because of the narrow temperature range in which $BiFeO_3$ stabilizes and there are a number of other phases of Bi and Fe, which appear if the temperature is not controlled accurately. Hence, the major bottlenecks of making $BiFeO_3$ powder lie in: i) synthesizing phase pure material and ii) getting highly resistive $BiFeO_3$ ceramics with low leakage current.
d) In solid state route $BiFeO_3$ phase formation is controlled by diffusion of $Bi_2O_3$ into $Fe_2O_3$ particle.
e) Wet chemical method is useful in synthesizing $BiFeO_3$ with least amount of impurity with control of particle size. Hydrothermal method is a useful technique for preparation of $BiFeO_3$ powder at low temperature (around $200^oC$) and particle size also can be controlled in an effective manner.
f) Polymer assisted hydrothermal synthesis is a useful technique for preparation of $BiFeO_3$ nanoparticle. But there is no literature available on sintering and electrical property of this nanoparticle.
g) $BiFeO_3$ in nano-crystalline form shows enhanced magnetization and superparamagnetism correlated with decreasing diameter. This is thought to be due to the large fraction of uncompensated spins from the surfaces of the nanocrystals.
h) Conventional sintering and rapid liquid phase sintering of $BiFeO_3$ was described, where the sintered density could not be achieved above 92% of the theoretical density. High vapour pressure of bismuth containing compounds can lead to neck growth without densification by evaporation-condensation mechanism. Rapid sintering is a technique allowing a very high heating rate at high temperatures which minimizes bismuth evaporation and maintaining stoichiometry.
i) It was observed that partial substitution of A-site cation in $BiFeO_3$ by lanthanide elements (La, Sm, etc) leads to improved ferroelectric properties and magnetization. Compared to Lanthanum, samarium will be effective as it has much lower ionic radius than Bismuth.

It is understood from the summary of literature review that need of the hour is to prepare nanosize $BiFeO_3$ powder with least amount of impurity phase that can be sintered to high density. Doping with suitable ion is required to improve the magnetic property of $BiFeO_3$.

## 3.2. Objective:

Our objective is to synthesize $BiFeO_3$ with least amount of impurity phase by hydrothermal technique at low temperature. To study whether particle size can be controlled by using polymer.

To prepare $BiFeO_3$ powder by solid state technique where initial oxide components are nanosize.

To study the densification behavior of synthesized powder by conventional sintering and microwave sintering technique.

To study the effect of samarium doping on phase formation, sintering behavior and microstructure and density of sintered ceramics.

To study the dielectric property of sintered ceramics.

# Chapter 4

# Experimental Procedure

## 4. Experimental Procedure:

In the present work, bismuth ferrite ($BiFeO_3$) and samarium doped $BiFeO_3$ was synthesized by hydrothermal route and solid state route.

## 4.1. Powder Preparation:

### 4.1.1. Hydrothermal Technique:

1. Preparation of 0.2M bismuth nitrate solution:
   0.2M $Bi(NO_3)_3$ solution was prepared by dissolving required amount of $Bi(NO_3)_3.5H_2O$ [MERCK, GR] in 120 ml nitric acid. Then the solution was diluted with deionized water. The solution was then filtered by using Whatman 41 filter paper and stored.
   Strength of the solution was calculated by using the following formula:

$$M = (W*1000) / (m*V)$$

   Where, M = Molarity of solution,
   W = weight of starting material (in gm)
   m = molecular weight of starting material,
   V = Total volume (in ml)

2. Preparation of 0.2 M ferric nitrate solution:
   0.2 M $Fe(NO_3)_3$ solution was prepared by dissolving required amount of $Fe(NO_3)_3.9H_2O$ [Lobachemie, GR] in deionized water. The solution was then filtered by using Whatman 41 filter paper and stored. Strength of the solution was calculated by using above mentioned formula:

3. Preparation of KOH solution:
   Different concentration of KOH solution was prepared by using the above mentioned formula. Stoichiometric amount of KOH [Qualigens ExcelaR] pellets are weighed and dissolved in pre-heated deionized water.

Equimolar solution of 0.2M $Bi(NO_3)_3$ and 0.2M $Fe(NO_3)_3$ was taken and mixed properly in magnetic stirrer. KOH solution is prepared separately. The mixed solution was then added slowly in the KOH solution and stirred continuously. A brown coloured precipitate appears and pH of the solution was maintained around ~ 13, for the complete formation of hydroxide precipitate. The solution was kept under stirring for 1 hour. It was again ultrasonicated for 30 minutes. After ultrasonicating it was transferred to teflon coated autoclave [BERGHOF BR300 Reactor; 700 ml]. The autoclave was maintained at 150-200°C with soaking time 6-12 hr. It is then cooled to room temperature. The precipitate obtained was washed several times with deionized water and acetic acid to remove additional salts. It is then dried at at ~75° C, followed by grinding in agate mortar. The powder obtained is pressed at a pressure of 4 ton with dwell time of 90 seconds.

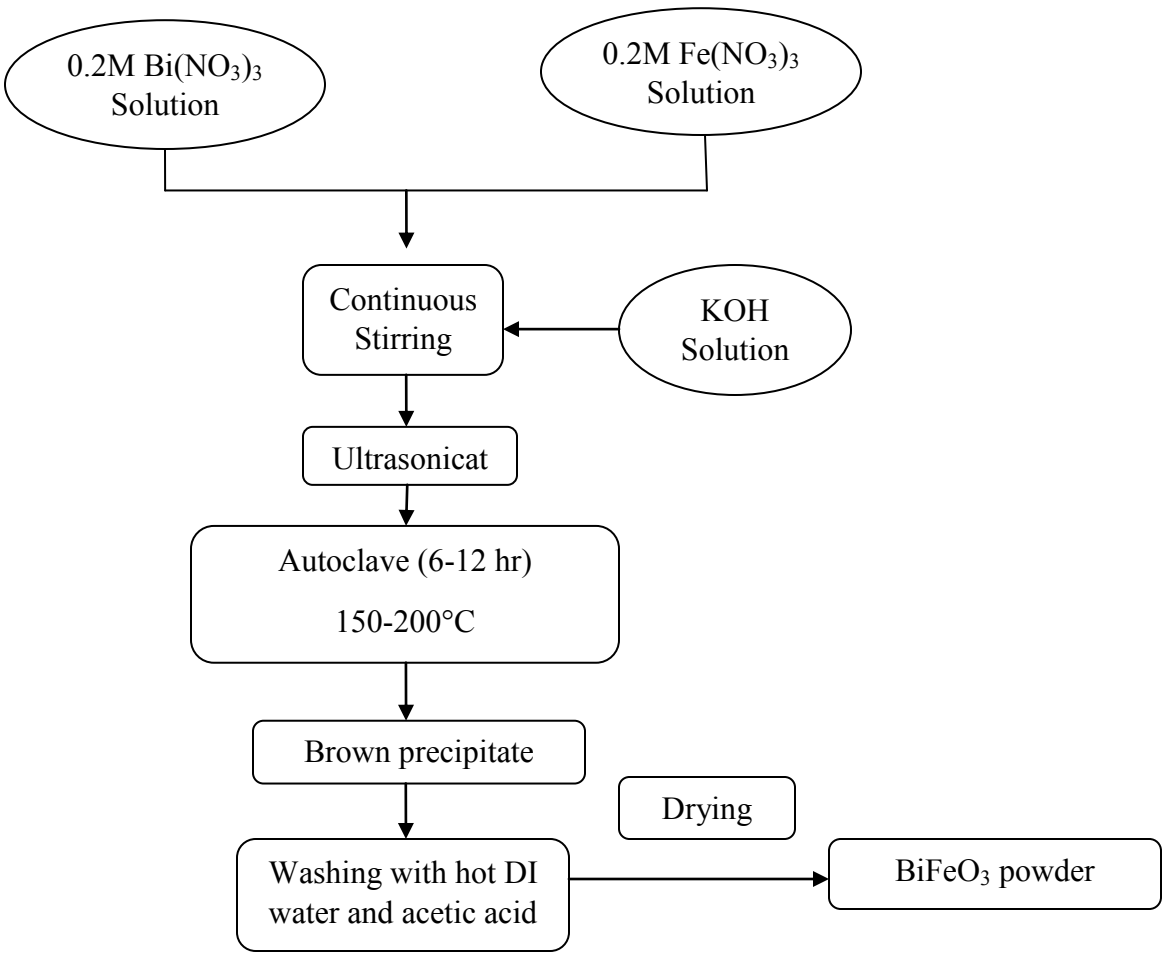


Fig 4.1 Flow chart for preparation of $BiFeO_3$ using hydrothermal technique

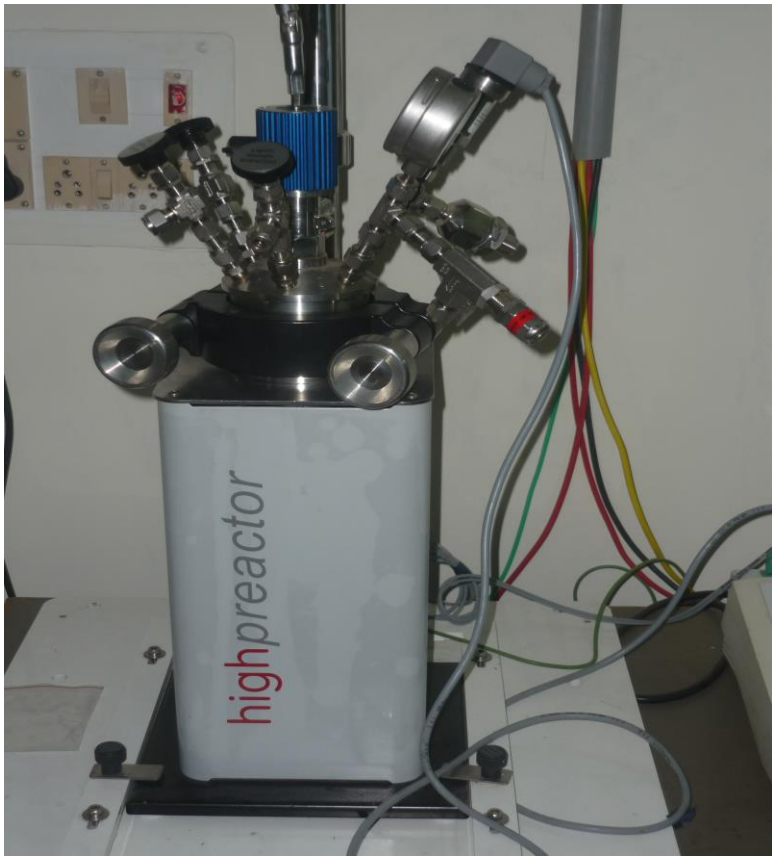


Fig 4.2 Photograph of Autoclave **[BERGHOF BR300 Reactor]** used in hydrothermal synthesis

### 4.1.2. Polymer Assisted Hydrothermal Technique:

Polymer assisted hydrothermal technique is very useful for synthesizing complex oxide nano-sized powders. Attempt was made to prepare BiFeO3 by polymer assisted hydrothermal technique keeping in mind the mechanism behind confinement of particle size (discussed in chapter 2). Initially 4M KOH solution was added to the mixture of $Bi(NO_3)_3.5H_2O$ and $Fe(NO_3)_3.9H_2O$ solutions. The precipitate was then washed with hot DI water to remove $NO_3^{-1}$ and $K^+$ ions. After obtaining pH up to 7.0, PVA (3.0 wt%) solution had been prepared by dissolving 3gms of PVA [Lobachemie] powder in hot DI water. The PVA solution prepared was then added followed by addition of 7M KOH solution, while continuously stirring the solution. The solution was ultrasonicate for 30 minutes and then transferred to an autoclave [BERGHOF BR300 Reactor; 700 ml]. The autoclave is maintained at 200°C and 15 bar pressure which soaking time ranging from 09 - 18 hours. It is then cooled to room temperature. The precipitate prepared is washed with DI water and acetic acid followed by drying.

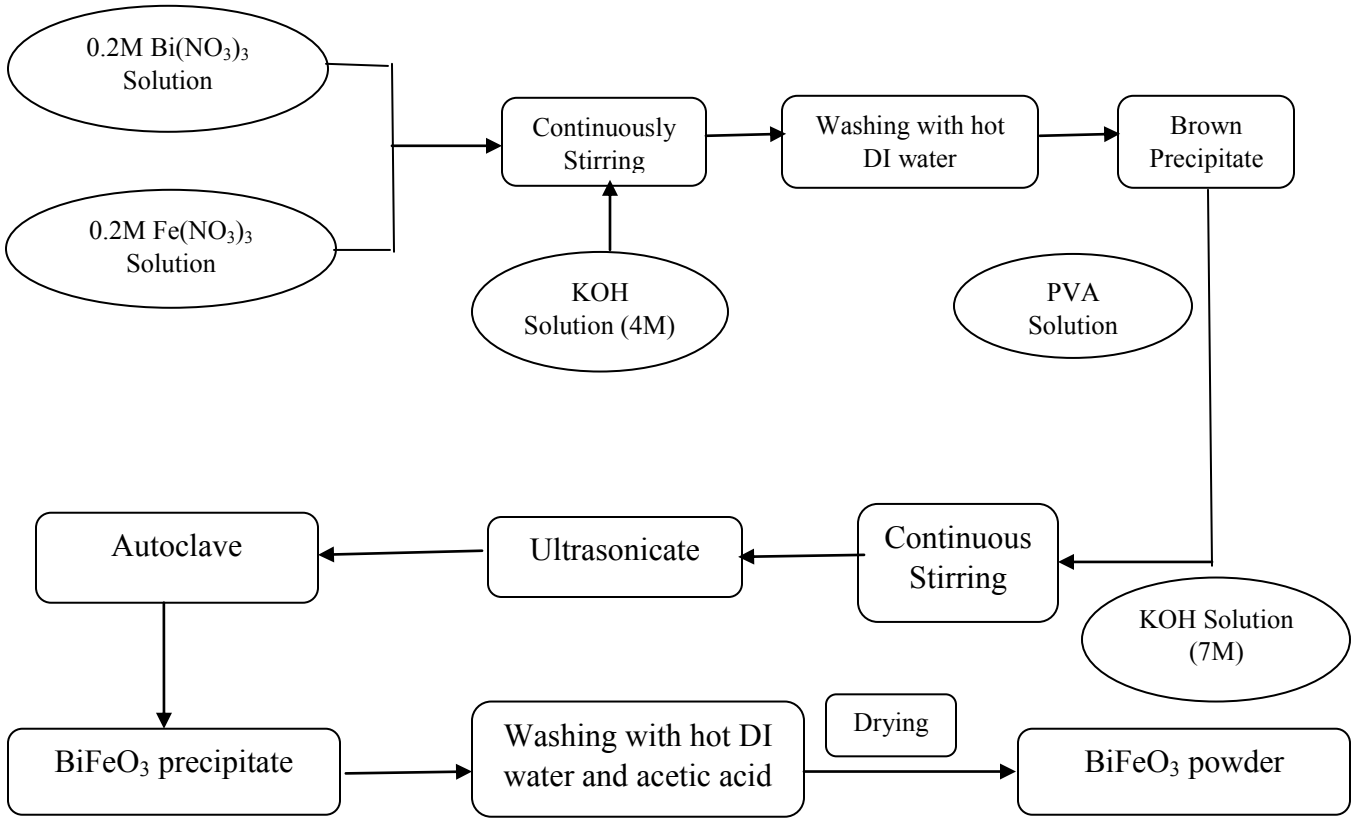


Fig 4.3 Flow chart for preparation of $BiFeO_3$ using hydrothermal technique using PVA as an additive

### 4.1.3. Samarium doped $BiFeO_3$ synthesis using hydrothermal technique:

Hydrothermal technique had also been used to synthesize samarium doped $BiFeO_3$ ($Bi_{1-x}Sm_xFeO_3$) powders. For $Bi_{1-x}Sm_xFeO_3$ synthesis, Samarium acetate (Alfa Aser) had been used as a samarium source. Depending upon the concentration of Sm, stoichiometric amount of samarium acetate required has been calculated while keeping the concentration of $Bi(NO_3)_3$ solution and $Fe(NO_3)_3$ solution same as before. The calculated values are as follows:

For x=0.05, Amount of Samarium acetate required = 0.32749gm;

For x=0.10, Amount of Samarium acetate required= 0.65498gm;

For x=0.125, Amount of Samarium acetate required= 0.818725gm.

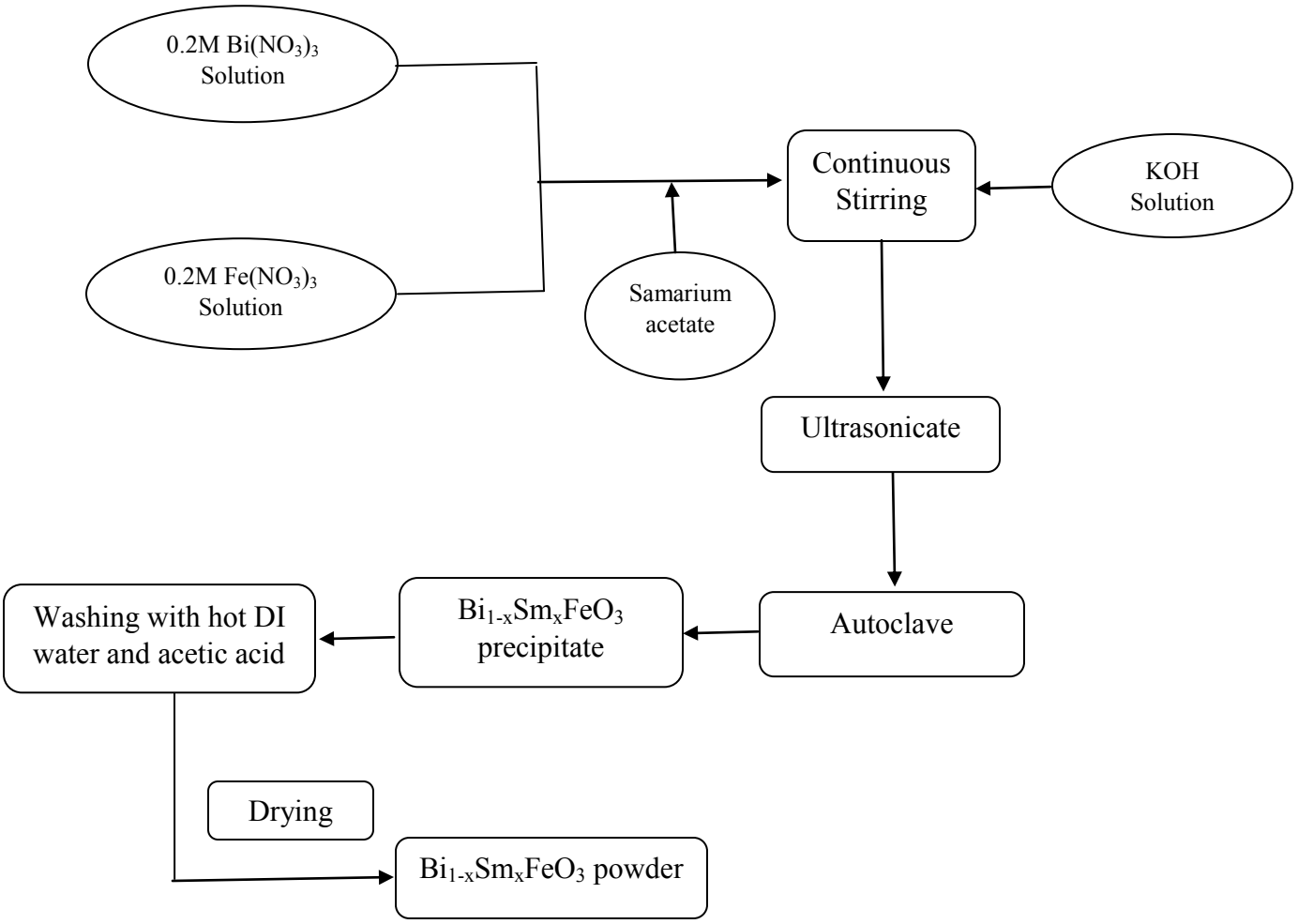


Fig 4.4 Flow chart for preparation of $Bi_{1-x}Sm_xFeO_3$ using hydrothermal technique

### 4.1.4. **Solid State Synthesis**:

$BiFeO_3$ had also been prepared by using solid state technique. Stoichiometric amount of $Bi_2O_3$ (Sigma Aldrich Chemicals Ltd., India, 99.8%, 90-210nm particle size), $Fe_2O_3$ (Sigma Aldrich Chemicals Ltd., India, particle size < 50nm) has been taken and pot-milled for 12 hours, using 2-propanol as a liquid medium. The milled power is then dried and grinded, followed by calcination at 500°C, 750°C and 820°C for 1hr, the calcined powder is grinded again and pressed to prepare pellet using PVA as a binding agent. The green pellets were then sintered using conventional as well as microwave sintering technique.

For 5gm $BiFeO_3$ powder synthesis using solid state route,

Amount of $Bi_2O_3$ powder required = 3.7238gm.

Amount of $Fe_2O_3$ powder required = 1.276gm.

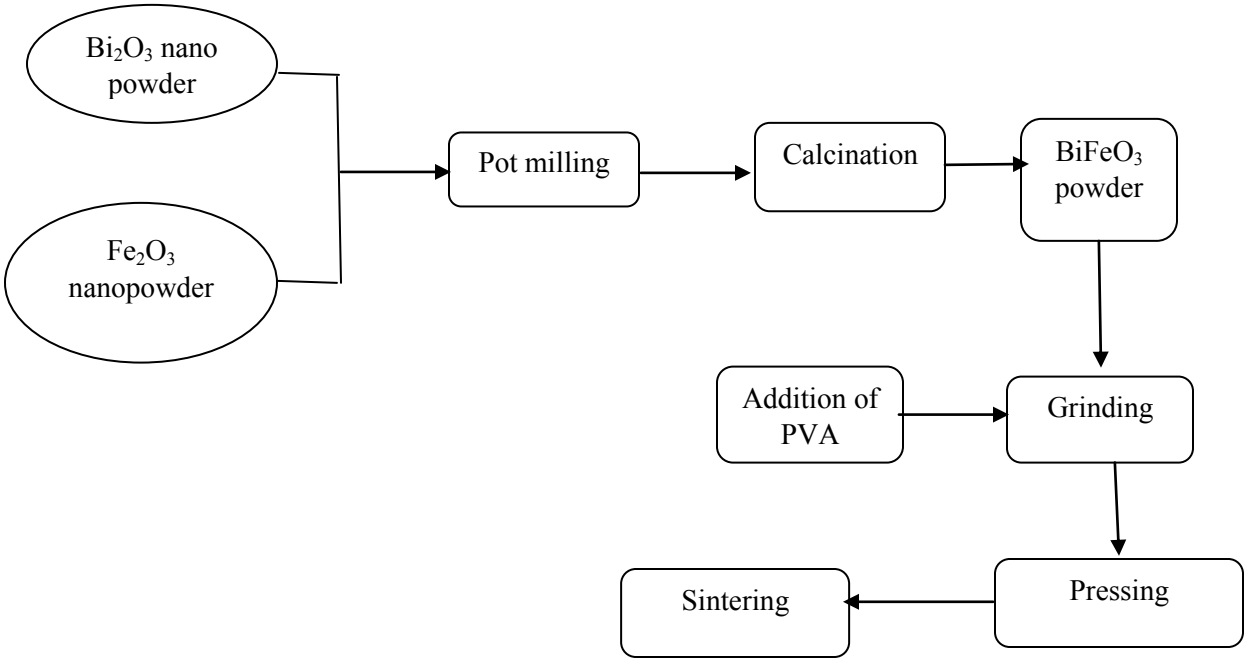


Fig 4.5 Flow chart for preparation of $BiFeO_3$ powder and sintered pellet using solid state synthesis route

### 4.1.5. Synthesis of $Bi_{1-x}Sm_xFeO_3$ using Solid state synthesis route:

Sm- doped $BiFeO_3$ ($Bi_{1-x}Sm_xFeO_3$) has been synthesis by solid state synthesis route. According to ref [5], the stoichiometric amount of $Bi_2O_3$ (Sigma Aldrich Chemicals Ltd., India, 99.8% pure, 90-210nm particle size), $Fe_2O_3$ (Sigma Aldrich Chemicals Ltd., India, particle size < 50nm) and $Sm_2O_3$ (lobachemie limited) has been taken and pot-milled for 12 hours, using 2-propanol as a liquid medium. The milled power was then dried and grinded, followed by calcination at 500°C for 1hr and 6hr, the calcined powder was grinded again and pressed to prepare pellet using PVA as a binding agent. The green pellets were then sintered using conventional as well as microwave sintering technique

For 5gm of $Bi_{1-x}Sm_xFeO_3$ synthesis using solid state route:

i. When x = 0.5,

   Amount of $Bi_2O_3$ powder required = 3.5711gm.

   Amount of $Fe_2O_3$ powder required = 1.2883gm.

   Amount of $Sm_2O_3$ powder required = 0.1407gm.

ii. When x = 0.10,

   Amount of $Bi_2O_3$ powder required = 3.415gm.

   Amount of $Fe_2O_3$ powder required = 1.301gm.

   Amount of $Sm_2O_3$ powder required = 0.2840gm.

iii. When x = 0.125,

   Amount of $Bi_2O_3$ powder required = 3.3365gm.

   Amount of $Fe_2O_3$ powder required = 1.3068gm.

   Amount of $Sm_2O_3$ powder required = 0.3567gm

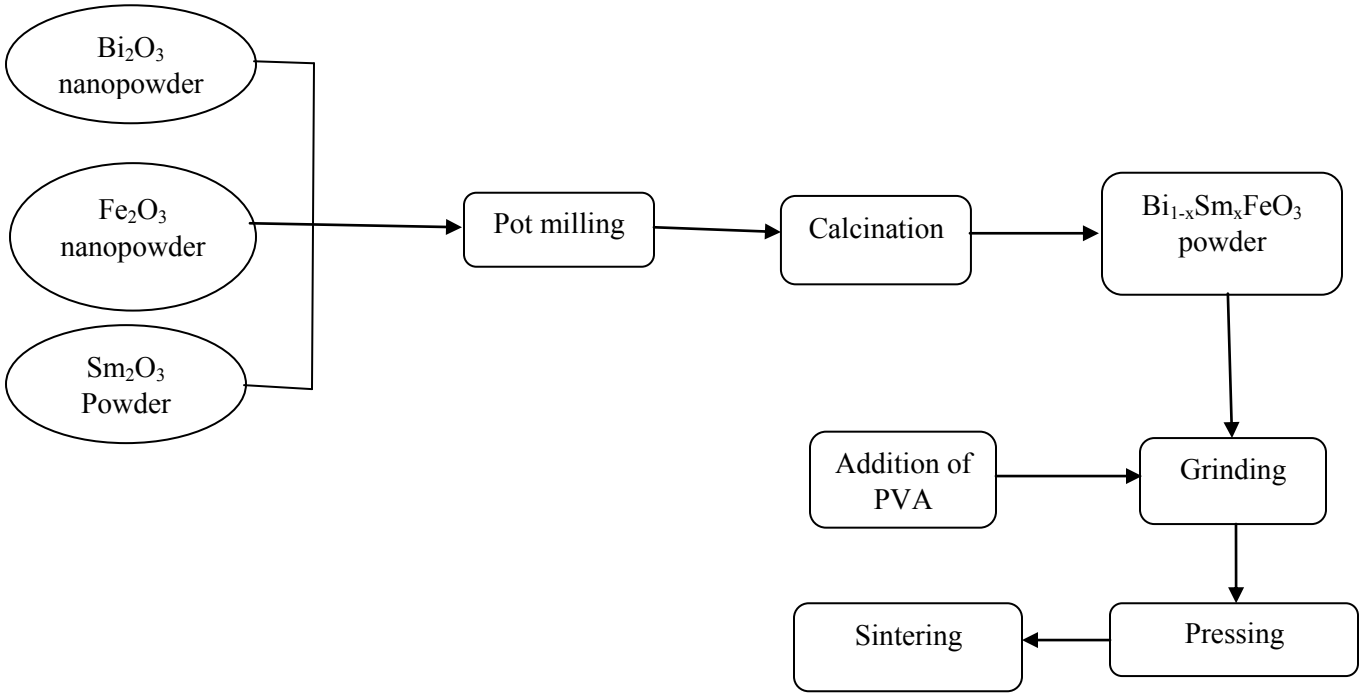


Fig 4.6 Flow chart showing formation of $Bi_{1-x}Sm_xFeO_3$ using solid state synthesis route

### 4.2. Preparation of Bulk Sample:

$BiFeO_3$ powders calcined at different temperature were mixed with 3 wt. % PVA (Poly Vinyl Alcohol) binder with the help of agate and mortar. The powder mixed with binder was compacted to give a desired shape. The mixed powders were pressed uniaxially in a HC-HCr die into cylindrical pellets (12 mm dia). The uniaxial pressing was done at 4 ton in a hydraulic press (4T,carver Inc ,USA) with holding time of 90 seconds for pressing of each sample.

### 4.3. Sintering:

Sintering was carried out by two different techniques; conventional and microwave sintering. For conventional sintering, Nabertherm electrically heated furnace (Model no LT5/13) was used at 820°C for 1hr whereas for microwave sintering, microwave furnace (VB Ceramic Consultants) was used at the temperature ranging from 800-850°C with 5-10 minutes soaking.

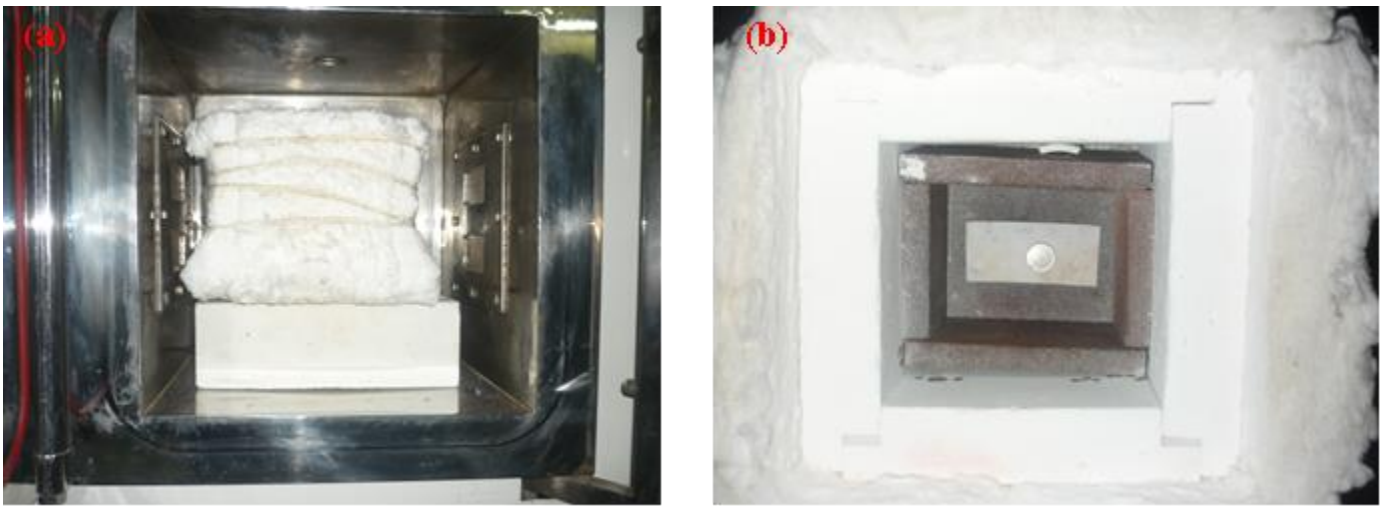


Fig 4.7 (a) Microwave Furnace (**VB Ceramic Consultants**) used in microwave sintering
(b) Top view of the zircar box containing succeptor and sample

### 4.4. Phase Identification:

The phases developed in the powder synthesized were identified by using X-ray diffraction technique (Philips Pan analytical, Netherland) using Ni filter and with Cu $K_\alpha$=1.54 A°. The generator current and voltage were set at 30 mA and 35KV, respectively. The samples were scanned in the 2Θ ranging from 15° to 80° in continuous scan mode. The scan rate was fixed at

3°/min. The search match facility available with Philips X'pert high score software has been used to identify the phases present in the sample.

The crystallite size of the prepared powders were calculated from X-ray line broadening using the Scherrer's equation as follows:

$$t = \frac{0.9\lambda}{\mathrm{B}\cos\theta}$$

Where, t = crystallite size;

λ = wavelength of the radiation;

Θ = Bragg's angle and

B = full width at half maximum

### 4.5. Particle size analysis:

The particle size analysis has been carried out by dispersing $BiFeO_3$ powders in deionized water and then sonicated using the ultrasonic probe to break the agglomerates. Then the particle size had been measured by using computer controlled particle size analyzer [ZETASIZER, Nanoseries (Malvern Instruments Nano ZS)].

### 4.6. Powder surface area measurement:

The powders were dried in an oven at 100°C for 12 hours before surface area measurement. BET (Brunauer, Emmett and Teller) surface area was measured using 5 point method by AUTOSORB 1, Quantachrome. The average particle size was estimated by assuming that all the particles were having the same spherical shape and size.

The average particle diameter, D (in nm), is given by:

$$D = \frac{6000}{\mathrm{S_{sp}} * \rho}$$

Where, $S_{sp}$ is the specific surface area in $m^2/gm$

ρ is the true density in $gm/cm^3$.

### 4.7. Thermal decomposition behavior:

Thermal behavior of the sample was studied using Netzsch, STA 449C. The DSC/TG patterns were collected as a function of temperature up to 820°C under $N_2$ atmosphere. The heating rate was maintained at 10°C/min.

### 4.8. Density measurement:

Archimedes principle has been used to measure the density of sintered sample. Kerosene has been used as the immersion liquid. The following equation was used to measure the density of sintered sample:

$$BD = \frac{D * \rho_s}{W - S}$$

Where, D = Dry weight of the sample,

$\rho_s$ = Density of kerosene,

W = Soaked weight,

S = Suspended weight.

### 4.9. Densification study of powder compact:

Shrinkage behavior of the green body and thermal expansion of sintered bar shaped samples had been investigated by NETZSCH dilatometer model DIL 402 C. The bar samples having length 15 mm and thickness up to 6 mm had been used for dilatometer experiment. The heating rate have been maintained at 10°C/min. The measurement had been carried out from room temperature upto 800°C.

### 4.10. Microstructural analysis:

Microstructure of sintered samples were observed using Scanning Electron Microscope (JEOL - JSM 6480LV).

### 4.11. Dielectric Measurement:

For dielectric measurement samples have been prepared by electroding with silver paste. The silver paste coated samples were cured at 500°C for half an hour. Dielectric measurement was

carried out using HIOKI-3532 LCR meter. The frequency range for the dielectric measurement was varied in the range of 100 Hz to 1MHz.

# Chapter 5

# Results and Discussion

## 5. Results and Discussion

### 5.1 Powder synthesis by hydrothermal method

#### 5.1.1. Phase analysis of $BiFeO_3$

Fig 5.1 shows the XRD pattern of $BiFeO_3$ powders synthesized using different concentrations of KOH solution under hydrothermal treatment at 200°C for 6h. It was found that phase pure $BiFeO_3$ can be prepared at a 7M KOH concentration, with a rhombohedral distorted perovskite structure with space group R3c which matched with the JCPDS file 82-1254. The XRD peaks revealed that well crystallized $BiFeO_3$ could be obtained by hydrothermal method. It was also observed that for 6M and 8M KOH concentrations, an impurity peak of bismuth rich $Bi_{25}FeO_{40}$ was formed in addition to the major $BiFeO_3$ phase. It is suggested that appropriate amount of KOH is beneficial to refrain the formation of impurity phases and therefore growth of $BiFeO_3$ powder into a single phase perovskite structure. Moreover it may be the decrease in molar ratio of bismuth nitrate to iron nitrate which catalyzed the formation of secondary phases. The average crystallite size was calculated using Scherer's formula and was found to be 55 nm. The hydrothermal reaction was described by the process of dissolution and crystallization. The probable reaction for formation of $BiFeO_3$ can be written as follows **[1].**

$$Bi(NO_3)_2 + Fe(NO_3)_2 + 6KOH \rightarrow Bi(OH)_3 + Fe(OH)_3 + 6KNO_3$$

$$25Bi(OH)_3 + 3Fe(OH)_3 \rightarrow Bi_{25}FeO_{39} + Fe_2O_3 + 42H_2O$$

$$Bi(OH)_3 + Fe(OH)_3 \rightarrow BiFeO_3 + 3HO_2$$

$$Bi_{25}FeO_{39} + 12Fe_2O_3 \rightarrow 25\,BiFeO_3$$

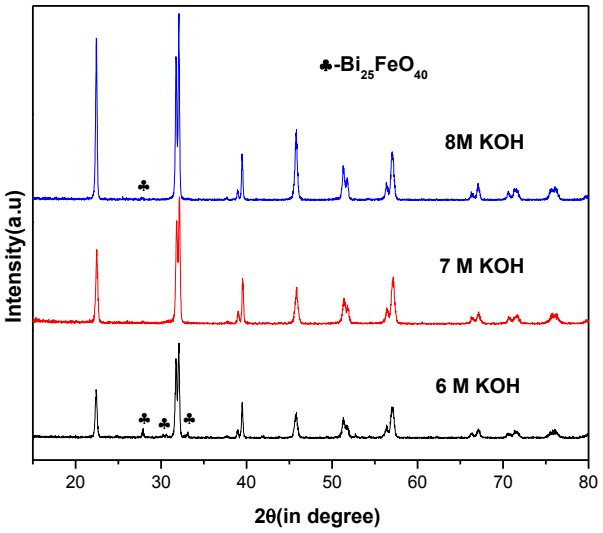


Fig 5.1 XRD pattern of $BiFeO_3$ powder synthesized by hydrothermal method using different concentrations of KOH.

### 5.1.2. Particle size and powder morphology

Fig 5.2 (a-b) shows the powder morphology and particle size of $BiFeO_3$ powder prepared by hydrothermal method. It has been observed that particles are agglomerated, irregular shape and some particles are spherical. The size of the agglomerated particles are 20-40 µm Individual particles are aggregation of small crystal of size 2-5µm (shown in Fig.5.2 (b)). The particles are formed by random aggregation of small crystal.

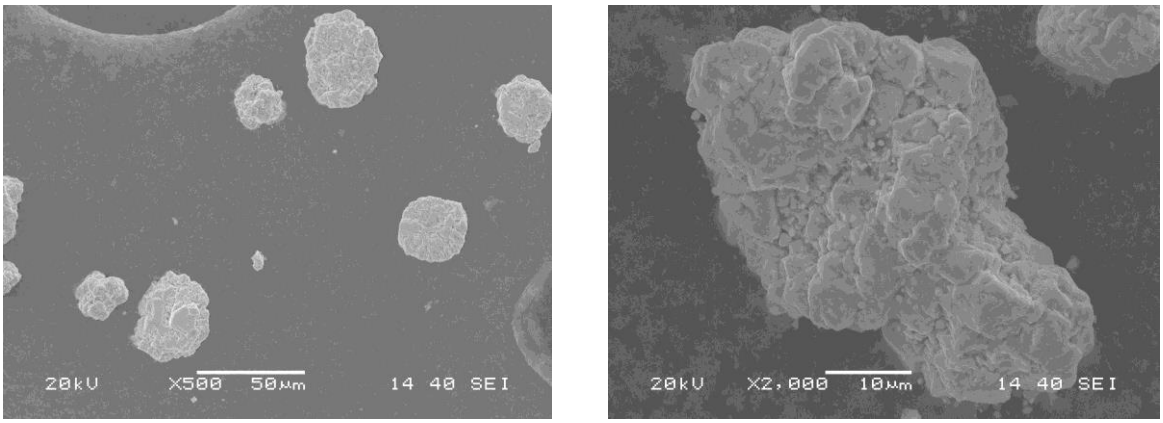


Fig 5.2 (a-b) SEM images of $BiFeO_3$ powder prepared by hydrothermal method using 7 M KOH at 200$^oC$ for 6h.

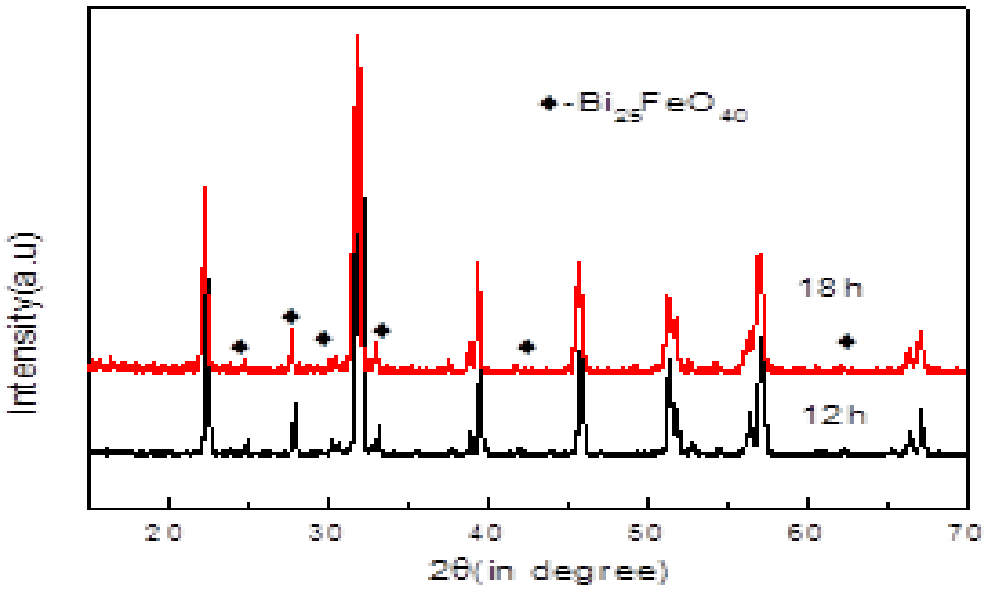


Fig 5.3 XRD pattern of $BiFeO_3$ powder synthesized by hydrothermal method using PVA.

Fig 5.3 shows the XRD pattern of $BiFeO_3$ powder synthesized by hydrothermal method using PVA as an additive, at 7M KOH. It could be observed that the addition of PVA in hydrothermal method, leads to an impurity peak of bismuth rich $Bi_{25}FeO_{40}$ phase. Very small amount of $BiFeO_3$ formation is also observed. It may be that PVA is restricting the reaction between $Bi_{25}FeO_{40}$ phase and $Fe_2O_3$. Hence, further study is required to understand the exact mechanism of getting the pure phase of $BiFeO_3$ in polymer assisted hydrothermal technique.

## 5.2. Sm doped $BiFeO_3$ by Hydrothermal method

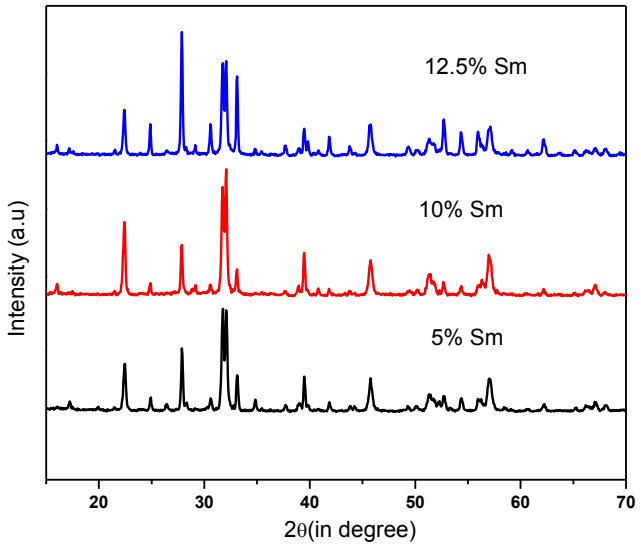


Fig 5.4 XRD pattern of Sm doped $BiFeO_3$ powder synthesized by hydrothermal method using 7M KOH.

Fig 5.4 shows the XRD patterns of Sm doped $BiFeO_3$ powders synthesized by hydrothermal method using 7M KOH. It can be observed that irrespective of doping of different concentrations of $Sm^{3+}$, no perovskite phase was formed. Rather, unreacted $Bi_2O_3$, $Fe_2O_3$ and bismuth rich $Bi_{25}FeO_{40}$ were observed in all compositions. It is surprising that at same condition with samarium addition phase pure powder could not be prepared. Further studies are required to understand the doping effect on phase formation of $BiFeO_3$ by hydrothermal method.

## 5.3. Solid state method

Fig 5.5 shows the XRD patterns of $BiFeO_3$ powder synthesized by solid state method using nanosize $Bi_2O_3$ and $Fe_2O_3$ as starting material. Surface area and particle size of oxide ingredients has been summarized in table 5.1. The mixed powders were calcined at different temperatures i.e. 500°C, 750°C and 820°C. It can be observed that with the increase in calcination temperature, the crystallinity of the powders increase. At 500°C, the impurity phases of $Bi_2Fe_4O_9$ and $Bi_{25}FeO_{40}$ were observed. It indicates that the $BiFeO_3$ is forming through the intermediate

phase of $Bi_2Fe_4O_9$ and $Bi_{25}FeO_{40}$.The impurity peak decreases with increasing calcination temperature. At 820°C, major phase is $BiFeO_3$ but very small amount of bismuth rich $Bi_{25}FeO_{40}$ was observed. The crystal structure is a rhombohedral distorted perovskite structure with space group R3c which matches with the JCPDS file 82-1254. The approximate fraction of BFO phase in the samples was determined from the XRD peak intensities using the relation: BFO% ≈ Imax (BFO)/[Imax(BFO) + Imax(second phase**)] [2].** The phase purity was found to be 92% and 95% for the $BiFeO_3$ ceramics calcined at 750°C and 820°C, respectively. The Average crystallite size was calculated using Scherer's formula and was found to be 60 nm and 73nm when the powders were calcined at 750°C and 820°C, respectively. It was found that with increase in calcination temperature, the crystallite size increases. The surface area of the 500°C calcined powder is 4.46 m2/g and corresponding particle size is 160nm which is lower than $Bi_2O_3$ particle (0.5 µm) and much higher than $Fe_2O_3$ particle (36 nm). It indicates that the diffusion of the Bi ions throughout the iron oxide particles controls the formation of $BiFeO_3$.

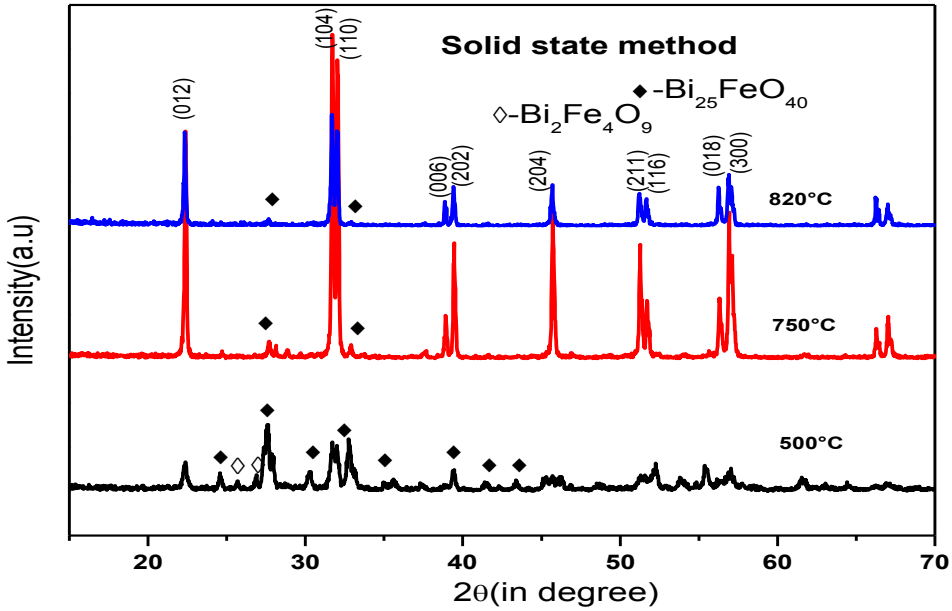


Fig5.5. XRD pattern of $BiFeO_3$ powder synthesized by solid state method using nano $Bi_2O_3$ and $Fe_2O_3$ stating material.

| Material | Surface area($m^2/g$) | Particle size (nm) |
|---|---|---|
| $Bi_2O_3$ | 1.361 | 516nm |
| $Fe_2O_3$ | 34.13 | 36nm |
| $BiFeO_3$ | 4.46 | 160nm |

Table 5.1 BET surface area and equivalent particle size calculated from BET surface area of stating raw material and precursor powder.

## 5.4. Sm doped $BiFeO_3$ by Solid state method

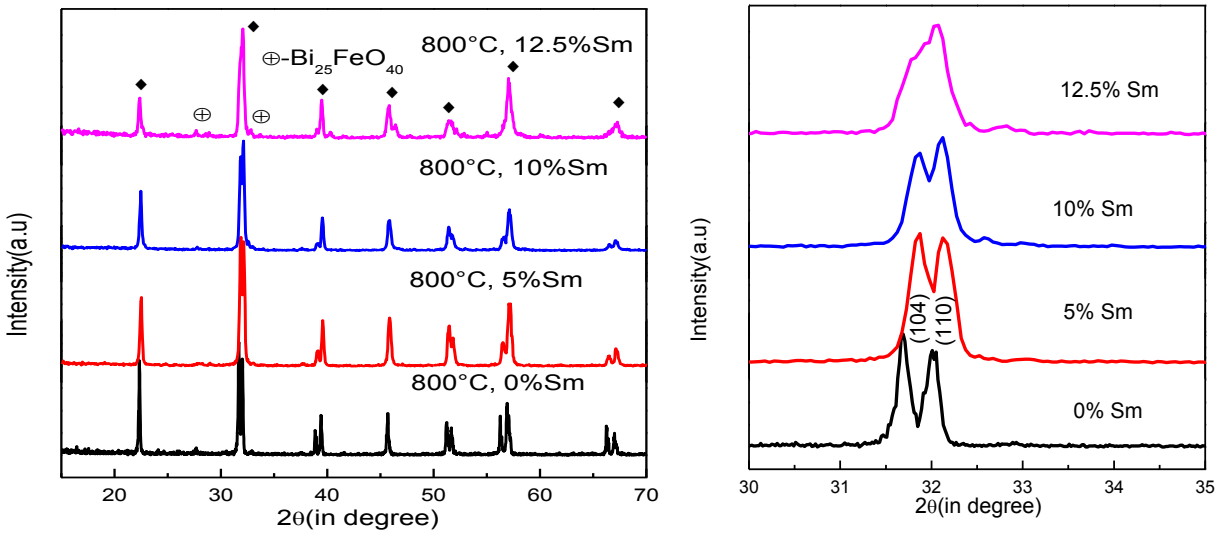


Fig 5.6 XRD pattern of (a) Sm doped $BiFeO_3$ powder synthesized by solid state method (b) (1 0 4) and (110) peak coalescence with increase in samarium content.

Fig 5.6 shows the XRD patterns of Sm doped $BiFeO_3$ powder synthesized by solid state method. The Sm doped $BiFeO_3$ powders were calcined at 800°C. With increase in Sm content, the

intensity of $Bi_{25}FeO_{40}$ impurity decreases. The phase purity was found to be 99% for 10 mol% of Sm doped $BiFeO_3$ ceramic. Higher purity in samarium doped sample could be attributed to higher ionic bond strength of Sm–O than the Bi–O bond. Enthalpy of formation ($\Delta H_f$) is dependent on bond energy which becomes more negative as the bond strength increases. This will make the $\Delta G_f$ more negative because entropy change is positive due to random replacement of Bi–O bond with Sm–O **[3]**. At higher concentration of samarium addition (12.5 mol%) produces more impurity phase which may be due to change in structure.

Fig. 5.6 (b) shows that pure $BiFeO_3$ ceramic shows two clear peaks corresponding to (104) and (110), while with increase the Sm doping; these two peaks show a trend to coalescence and form a broad peak. The crystal structure of $BiFeO_3$ is a rhombohedral distorted perovskite structure with space group R3c. The crystal structure is changing from rhombohedral to tetragonal symmetry with increase in the Sm content **[2, 4]**. Moreover, it is clear that the position of diffraction peaks of the Sm doped $BiFeO_3$ has shifted to higher angle with increase in Sm content and it is caused by the distortion of crystal lattice induced by the substitution of $Sm^{3+}$( radius=0.958 Å) by larger $Bi^{3+}$ (radius=1.030 Å).

### 5.5. Shrinkage Behavior of $BiFeO_3$

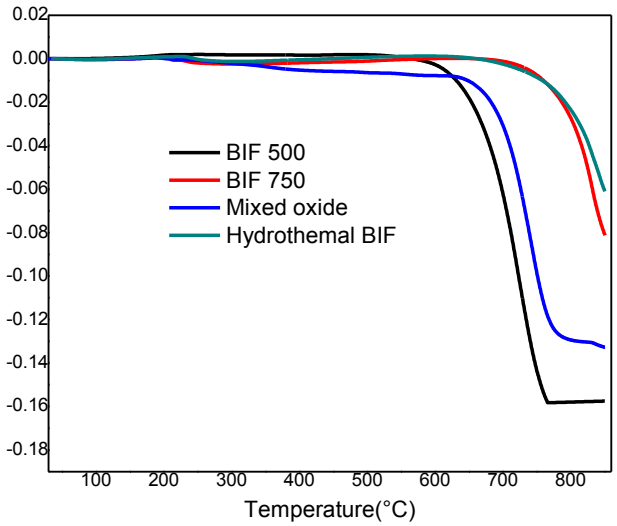


Fig 5.7 Linear shrinkage of powder compact synthesized by solid state method and hydrothermal method.

| **Method** | **Onset temperature** | **Maximum Shrinkage (%)** |
|---|---|---|
| BIF500 | 627°C | 16 |
| BIF750 | 744°C | 08 |
| BIF Mix oxide uncalcined | 664°C | 13 |
| BIF-HM<br><br>Hydrothermal Method | 729°C | 06 |

Table 5.2 Onset temperature and maximum shrinkage of BiFeO3 prepared by solid state method and hydrothermal method.

Fig 5.7 shows the linear shrinkage as a function of temperature for $BiFeO_3$ powder prepared by solid state method at different calcination temperatures and hydrothermal method. It can be

observed that lower calcination temperature (500°C) prepared powder shows maximum shrinkage with narrow temperature range (630-750°C). Hydrothermal method and higher calcination temperature (750°C) of $BiFeO_3$ show minimum shrinkage of the sample. The onset temperature and maximum shrinkage are shown in the table 5.2.The sinterablily of the powders depend upon the different properties of the powders in terms of particle size, composition and surface area. It can be seen that lower calcination temperature gives higher surface area which is the driving force for maximum shrinkage of the green pellets over narrow temperature range and hence a sintered density as high as 95% of theoretical density could be obtained in this sample. The hydrothermal method consists of large agglomerates, which is not favorable for achieving high sintered density. Hence the low temperature calcined powder (500°C) was considered for further studies which obtained by solid state route.

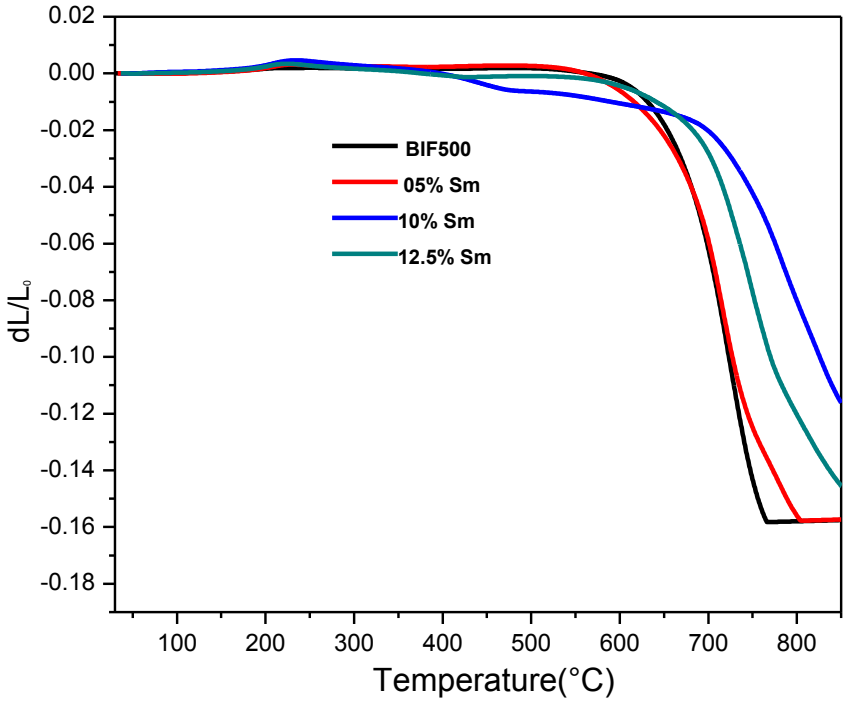


Fig 5.8 Linear shrinkage as a function temperature of Sm doped $BiFeO_3$ ceramic synthesized by solid state method.

Fig 5.8 shows the linear shrinkage as a function of temperature for Sm doped $BiFeO_3$ ceramics synthesized by solid state method. It can be observed that sintering process is strongly influenced by Sm/Bi ratio and controls the maximum shrinkage rate and onset of shrinkage. The sintering temperature increases with increasing content of Sm upto 10% and decreases afterwards. At

higher samarium content produces impurity phase which melts at lower temperature and produces higher shrinkage.

## 5.6. Density measurement

| Composition (solid state method) | Calcination temperature | Bulk density | Relative density |
|---|---|---|---|
| Conventional Sintering at 820°C/1h | | | |
| x=0 | 750°C/1h | 6.99 | 83 |
| x=0 | 500°C/6h | 7.96 | 94.56 |
| x=0.05 | 500°C/6h | 8.14 | 96.1 |
| x=0.10 | 500°C/6h | 7.96 | 94.56 |
| x=0.125 | 500°C/6h | 7.3 | 86 |
| Microwave Sintering at 850°C/5min | | | |
| x=0 | 750°C/1h | 7.6 | 90 |
| x=0 | 500°C/6h | 7.93 | 94.29 |
| X=0, 800°C/30 min | 500°C/6h | 7.96 | 94.56 |
| x=0.05 | 500°C/6h | 7.92 | 94 |
| x=0.10 | 500°C/6h | 7.85 | 93.7 |
| x=0.125 | 500°C/6h | 7.6 | 90 |
| Hydrothermal method Microwave Sintering of $BiFeO_3$ | | | |
| 800°C/30min | - | 6.13 | 72.97 |
| 825°C/30min | - | 6.25 | 74.32 |
| 850°C/30min | - | Melt | - |
| 850°C/5min | - | 6.73 | 80 |
| Hydrothermal method conventional Sintering of $BiFeO_3$ | | | |
| 800°C/1h | - | 6.10 | 72.6 |
| 850°C/1h | - | 6.51 | 77.5 |

Table 5.3. The bulk density and relative density of $BiFeO_3$ and Sm doped $BiFeO_3$ prepared by solid state method and hydrothermal method

The bulk density and relative density of $BiFeO_3$ and Sm doped $BiFeO_3$ prepared by solid state method and hydrothermal method are shown in Table 5.3. It can be observed that the bulk density and relative density were nearly constant with increasing Sm content up to 10% and decreases beyond that in both microwave and conventional sintering methods. It may be due to the higher impurity content in 12.5 mol% Sm in $BiFeO_3$. The reasonable density achievement at lower temperature may be attributed to very fine particle size of synthesized powders. But in hydrothermal method, the $BiFeO_3$ could only be sintered more than 80% of theoretical density by microwave sintering. It may be hard agglomerates that are not favorable for achieving high sintered density. It should be mentioned that microwave sintering significantly reduces firing time without hampering the density.

## 5.7. Microstructure of Sintered sample

### 5.7.1. Hydrothermal method

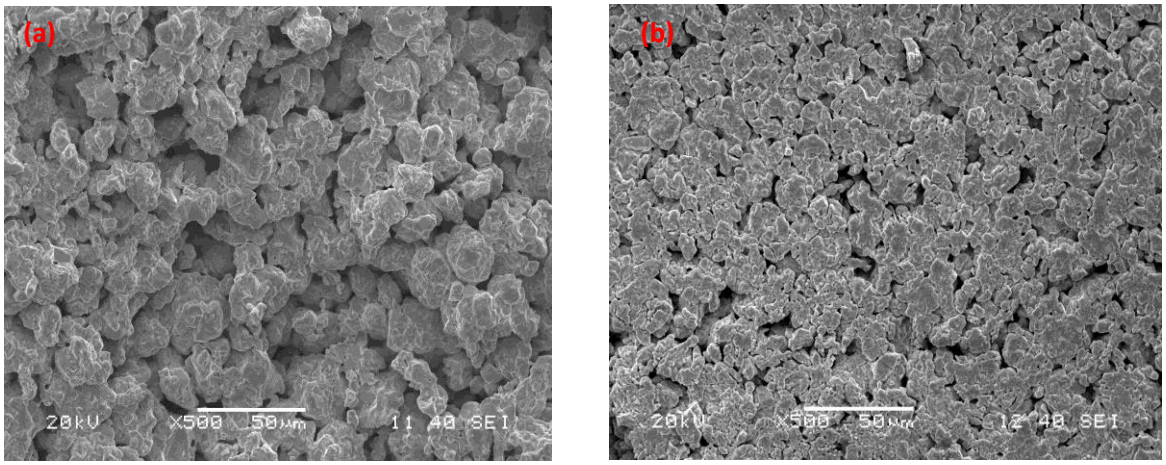


Fig 5.9. SEM microstructure of $BiFeO_3$ ceramic (a) conventional sintering 820°C for 1h (b) Microwave sintering 850°C for 5min prepared by hydrothermal method using 7 M KOH.

Fig 5.9 shows the SEM microstructure of $BiFeO_3$ ceramic sintered by different sintering methods. It can be observed that microwave sintered sample has significant amount of pores.

### 5.7.2. Solid state method

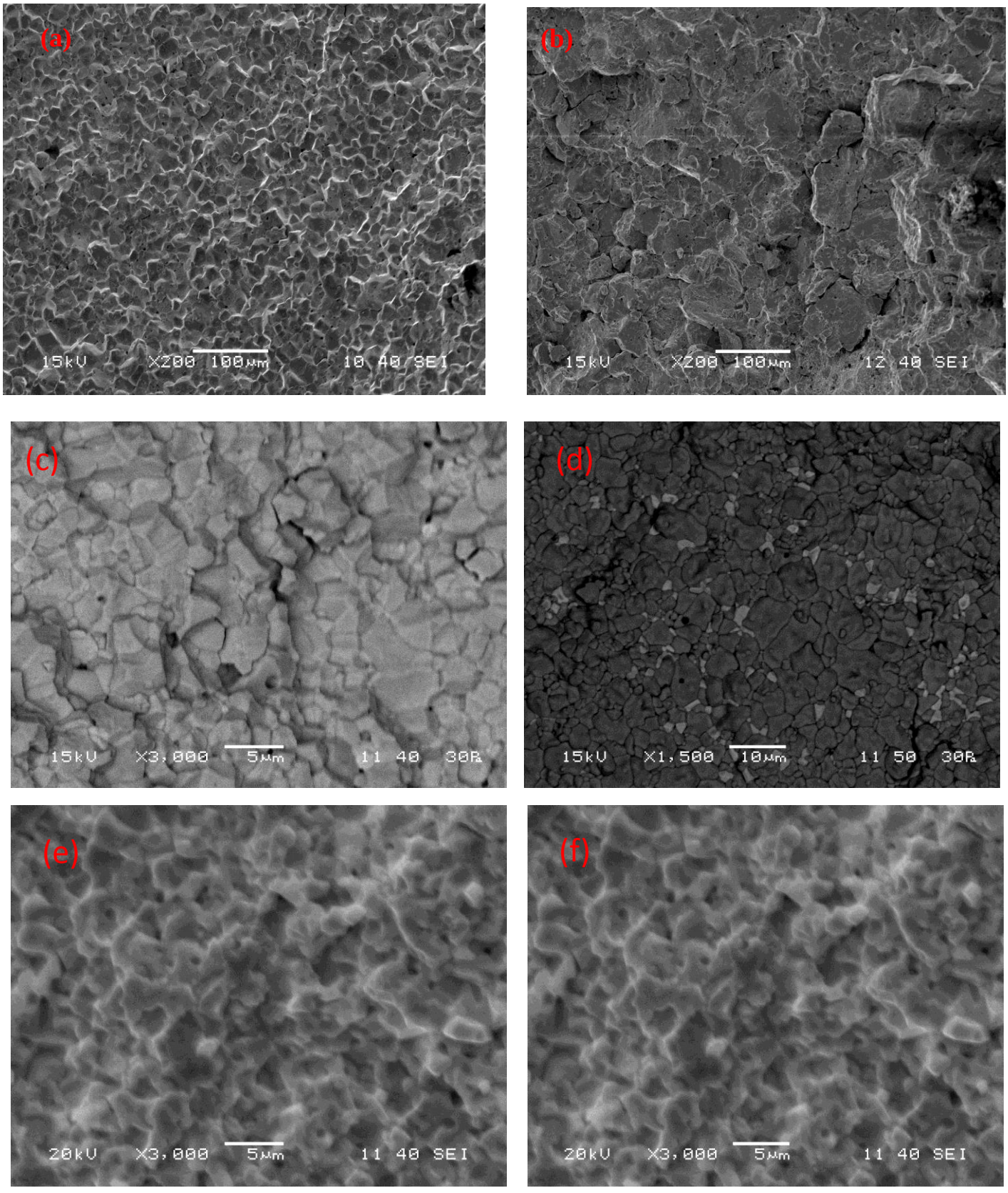

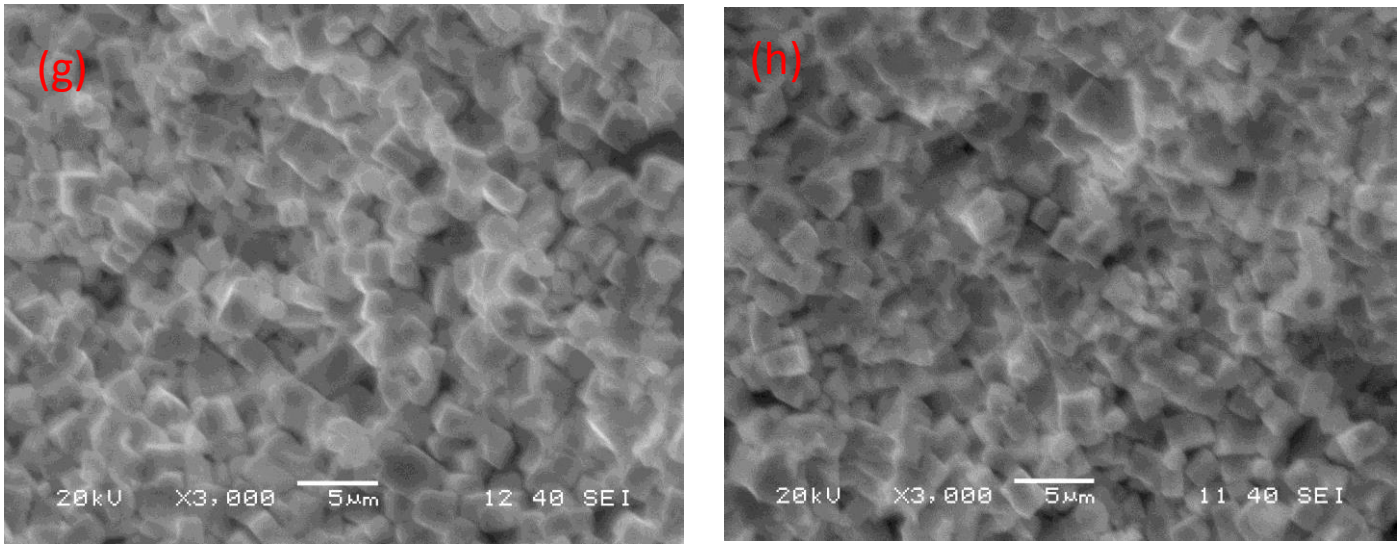


Fig 5.10. SEM microstructure of $BiFeO_3$ ceramic and Sm doped $BiFeO_3$ prepared by solid state method using different sintering method (a) x=0 (c) x=0.05(back scattered) (e) x=0.10 (g) x=0.125 by conventional method (b) x=0 (d) x=0.05(back scattered) (f) x=0.10 (h) x=0.125 microwave sintering.

| Composition | Conventional Method (Grain size µm) | Microwave sintering Method (grain size µm) |
|---|---|---|
| x=0 | 17.33-28.34 | 24.50-44.48 |
| x=0.05 | 2.198-4.01 | 3.35-5.08 |
| x=0.10 | 1.11-1.5 | 1.15-1.51 |
| x=0.125 | 1.511-2.38 | 1.63-2.78 |

Table 5.4 Comparison of grain size of the Microwave and Conventional sintering of $BiFeO_3$ and Sm doped $BiFeO_3$

The SEM micrographs of facture surface $BiFeO_3$ of different sintering methods was shown in Fig.5.10 (a) and (b). It can be observed that the microwave sintered $BiFeO_3$ shows larger grains compared to conventional sintered $BiFeO_3$. Dense microstructures were obtained in both the

sintering methods. The grain size is found to decrease with the increase in Sm content upto 10% and after that slightly increases. It means that Sm doping can suppress grain growth and lead to small grain sizes in the materials. The decrease in grain size may be attributed to the difference in the ionic radius of $Bi^{3+}$ and $Sm^{3+}$ion. Fig 12(b) & (d) shows the back scattered image of 5% Sm doped $BiFeO_3$. It can be observed that the smaller crystallites are observed in the SEM may be due to the presence of impurity ($Bi_{25}FeO_{40}$) phase which is also detected by XRD. The shape of the grains was changed to cuboidal with increasing Sm content (12.5%).The comparison of grain size of the Microwave and Conventional sintering of $BiFeO_3$ and Sm doped $BiFeO_3$ is shown in Table 5.4.

## 5.8. Dielectric measurement

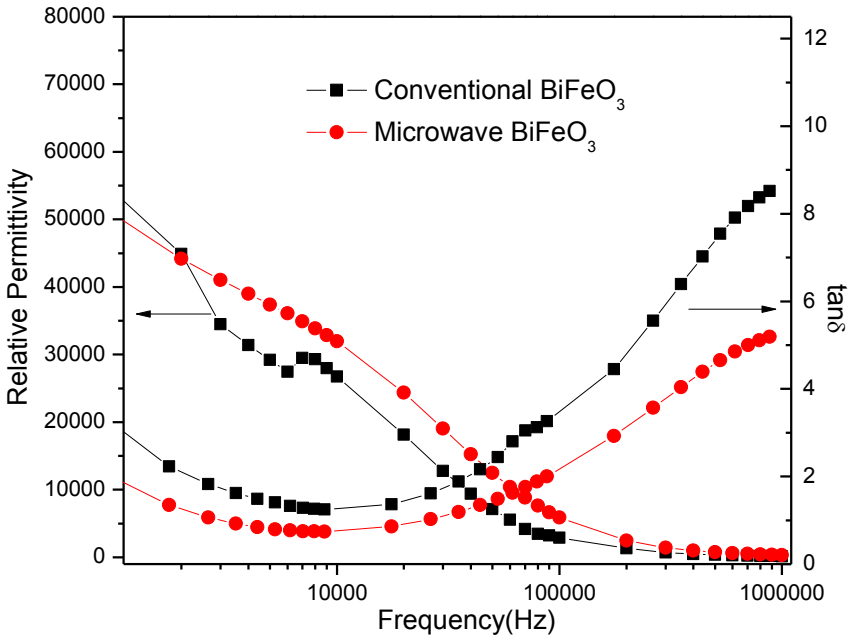


Fig. 5.11 Relative Permittivity and loss tangent with frequency of $BiFeO_3$ ceramics prepared by conventional and microwave sintering technique.

Fig. 5.11 shows the relative permittivity and loss tangent with frequency of $BiFeO_3$ ceramics prepared by sold state method using two different sintering technique conventional and microwave. It can be observed that microwave sintered sample has low loss compared to

conventional sintered sample. The dielectric constant of all the samples decreases as the frequency increases. Both the sample has significant dielectric loss. Space charge polarization at low frequency is responsible for high dielectic constant at low frequency. Moreover, it was observed that the relative permittivity of microwave sintered ceramics is larger than that of the conventional sintered ceramics. It can be attributed to the larger grain size microwave sintered ceramics.

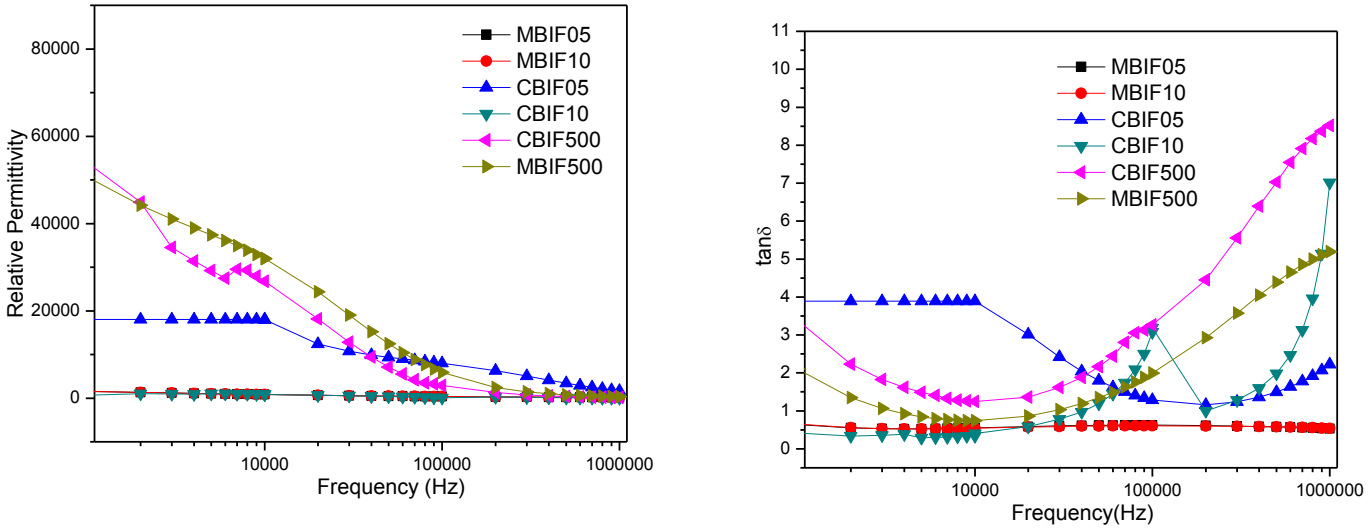


Fig. 5.12 Relative permittivity and loss tangent with frequency of $BiFeO_3$ and Sm doped $BiFeO_3$ ceramics prepared by conventional and microwave sintering technique.

Fig 5.12 shows the addition of samarium drastically reduces the frequency dispersion of BiFeO3 with low dielectric loss. It is discussed earlier samarium modification reduces impurity content and that may be the reason for reduction of dielectric loss. High loss in BiFeO3 may be attributed to oxygen vacancies and multivalent state in iron ions ($Fe^{3+}$ and $Fe^{2+}$) via the formation of shallow energy centers [5,6]. There is no significant change in dielectric property observed for Sm-doped $BiFeO_3$ densified by microwave and conventional sintering technique.

## Reference:


1. Xian-Zhi Chen, Zhong-Cheng Qiu, Jian-Ping Zhou, Gangqiang Zhu, Xiao-Bing Bian, Peng Liu, Large-scale growth and shape evolution of bismuth ferrite particles with a hydrothermal method, Materials Chemistry and Physics 126 (2011) 560–567.

2. Pyroelectric properties and electrical conductivity in samarium doped BiFeO3 Ceramics, Y.B. Yao et al. / Journal of Alloys and Compounds 527 (2012) 157– 162.

3. K.S. Nalwa, A. Garg, A. Upadhyaya. Materials Letters 62 (2008) 878–881.

4. Z. Wen, X. Shen, D. Wu, Q.Y. Xu, J.L. Wang, A.D. Li, Solid State Commun. 150,(2010) 2081.

5. Siwach P K, Singh H K, Singh J, Srivastava O N. Anomalous ferromagnetism in spray pyrolysis deposited multiferroic BiFeO3 films. Appl. Phys. Lett., 2007, 91: 122503.

6. Yuan G L, Or S W, Chan H L W, Liu Z G. Reduced ferroelectric coercivity in multiferroic Bi0.825Nd0.175FeO3 thin film. J.Appl. Phys., 2007, 101: 024106.

# Chapter 6

# Conclusions

## 6. Conclusions:

It can be concluded from the present work that hydrothermal technique can be a useful method to prepare single phase $BiFeO_3$ at 200$^oC$. KOH concentration has major role in achieving phase purity and particle morphology. Phase pure $BiFeO_3$ could be produced using 7 M KOH solution. It possesses a single phase perovskite structure with rhombohedral symmetry. It is found that particle size is in the range of 20-30 μm. But in hydrothermal method prepared $BiFeO_3$ could only be sintered upto 80% of theoretical density by microwave sintering. It may be hard agglomerates that are not favorable for achieving high sintered density.

We could not prepare phase pure powder by hydrothermal technique where poly vinyl alcohol (PVA) used as an additive to control the particle size. Further study is required to understand the mechanism of synthesis of $BiFeO_3$ nanoparticles at lower temperature by polymer assisted hydrothermal synthesis.

$BiFeO_3$ was also prepared by solid state method using nanosized $Fe_2O_3$ and $Bi_2O_3$. $BiFeO_3$ with lowest impurity content can be prepared above 800$^oC$. The powder could be sintered to 95% of theoretical density. Microwave sintered $BiFeO_3$ shows larger grains compared to conventional sintered $BiFeO_3$. Dense microstructure was obtained in both the sintering methods. Additional advantage of microwave sintering is that sintering could be completed within a short period of time. Microwave sintered $BiFeO_3$ has low dielectric loss compared to conventional sintered sample that may be due to lower defect concentration in sintered specimen. It is found that samarium (Sm) doping in $BiFeO_3$ significantly reduces the impurity content, grain size in sintered body and modifies crystal structure. With increase in Sm content, the phase purity was increased from 95% to 99%, upto 10% of Sm doping that may be attributed to higher Sm-O bond strength than Bi-O bond strength. The grain size was found to decrease with the increase in Sm content upto 10% of samarium addition and after that slightly increased. The decrease in grain size may be attributed Modification in grain boundary structure caused by $Sm^{3+}$ substitution (lower ionic radius of $Sm^{3+}$ 0.96 Å than $Bi^{3+}$ with 1.030 Å which dominates the microstructure evolution. Microwave sintered Sm doped $BiFeO_3$ shows larger grains compared to conventional sintered one. The dielectric loss decreases significantly with the increase of Sm content. Further study is required to check sintering at lower temperature which could improve the electrical property further without hampering the density.

## Future Work:

1) Measurement of magnetic property with temperature for pure $BiFeO_3$ and Sm-doped $BiFeO_3$.
2) To check sintering at lower temperature could improve the electrical property without hampering density much.
3) Understanding the mechanism of synthesis of $BiFeO_3$ nanoparticle at lower temperature by polymer assisted hydrothermal synthesis.